



**The Abdus Salam  
International Centre for Theoretical Physics**



**2268-14**

**Conference on Nanotechnology for Biological and Biomedical  
Applications (Nano-Bio-Med)**

*10 - 14 October 2011*

**Bio-Functional Inorganic Nanomaterials and Nanocomposites for Therapeutics and  
Diagnostics**

Sangeeta KALE

*Dept. of Applied Physics  
Defence Institute of Advanced Technology, Girinagar  
Pune 411025  
INDIA*



# Bio-Functional Inorganic Nanomaterials and Nanocomposites for Therapeutics and Diagnostics

**Sangeeta Kale**

*Department of Applied Physics  
Defence Institute of Advanced Technology,  
Girinagar, Pune, India*

Talk at ICTP-KFAS Conference on Nanotechnology for Biological and Biomedical Applications (Nano-Bio-Med) between 10-14 October, 2011

# The Team...



## Students:

- J. Mona (now post-doc, Taiwan)
- Shadie Hatamie (Ph.D. completed)
- **Rohini Kitture**
- Sandip Dhobale
- Nageswara Rao
- Ganesh Shitre
- **Anil Jadhav**
- Shreelekha Khatavkar
- **R. Rajagopal** (Ph.D. Prof Rao IITB)
- **Trupti Thite**
- **Anansa Ahmed**
- Londhe S.P.
- Shilpa Kasar

## Funding support:

University Grants Commission, UoP-  
ISRO, UGC-DAE-CSR, Department of  
Science and Technology (SERC, TSG,  
NanoMission) , DRDO

## Collaborators

- **S. B Ogale (NCL, Pune)**
- Beatrice Hannyer (Rouen, France)
- **Ding Jun & Dipak Maity** (NUS, Singapore)
- Sam Lofland (Rowan, NJ, USA)
- **S.D. Dhole (Pune University)**
- **R. Kaul-Ghanekar (IRSHA)**
- Ram J Chaudhary (UGC-DAE-CSR, India)
- D.M. Phase (UGC-DAE-CSR, India)
- **S.D. Kulkarni (NCL, Pune)**
- Suresh Gosavi (Pune University, India)
- **B.R. Chopade (Pune University, India)**
- B.B. Kale (C-MET, Pune, India)
- S. Datar & P.S. Alegaonkar (DIAT, India)
- P.S. Kulkarni (DIAT, Pune, India)
- Brigitte Pepin Donat (Grenoble, France)
- A. Ahmad & A. Prabhune (NCL, India)



## Recent Studies of functional nanomaterials used for healthcare applications:...

- Nanostructured oxide thin films as glucose sensing kit and amylase inhibitors.
- Co-Ni-O - amino acids, manganites for drug delivery and hyperthermia
- Iron oxide - Curcumin system for drug bioavailability, targeting and hyperthermia, antioxidants, tumor suppression / inhibitors
- Cobalt - curcumin for antimicrobial studies
- Polymeric and inorganic porous networks for drug encapsulation, release and storage : for medicinal patches
- ZnO Nanomaterials for water pollution control
- SnO<sub>2</sub> Nanomaterials for chemical and biological warfare diagnostics



## Other areas of work : Sensors and Devices

- Thin film heterostructures for device applications : manganite-semiconductors devices for magneto-electronics and spintronics
- Inorganic-organic complexes for DMS applications
- Nanostructured thin films for low field-magneto-sensing (LFMR) applications and miniaturized devices studies
- Newer methods to synthesise materials in nanoforms, using chelation approach (chemical) and high-power laser ablation tools
- Optical fiber based sensors : material manipulation or sensing materials deposition



## Focus during the talk ...

Different magnetic nanomaterials for applications in therapeutics and diagnostics

### ✓ Iron oxide - Curcumin system for:

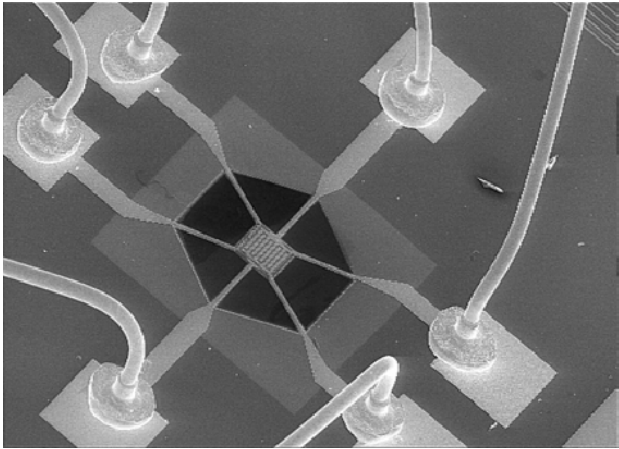
- Drug bioavailability
- Cancer Hyperthermia
- Tumor Suppression and Inhibition
- Antioxidants

### ✓ Nickel Cobaltite ( $\text{NiCo}_2\text{O}_4$ ) - amino acids conjugates for:

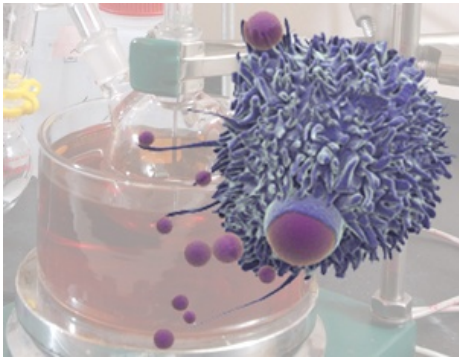
- drug delivery
- Cancer hyperthermia

### ✓ Transition temperature-tuned Manganite nanoparticles conjugated with proteins and biopolymers for:

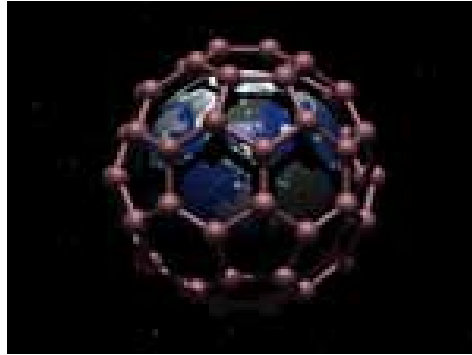
- Cancer hyperthermia
- Drug delivery



Biosensors



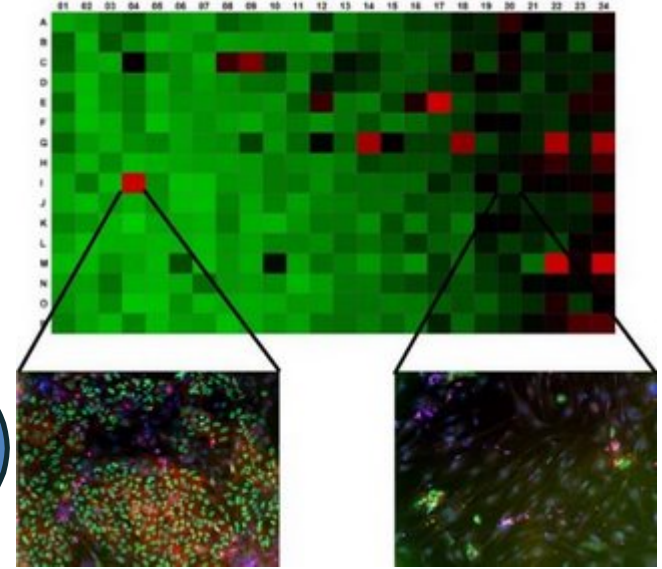
Nanoreactors



Drug encapsulators

**Nanoparticles in Therapeutics**

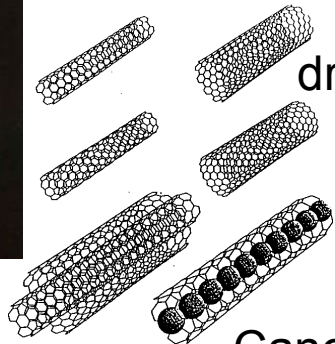
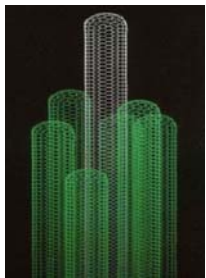
Cell labeling and imaging



MRI contrast agents

Tissue repairing

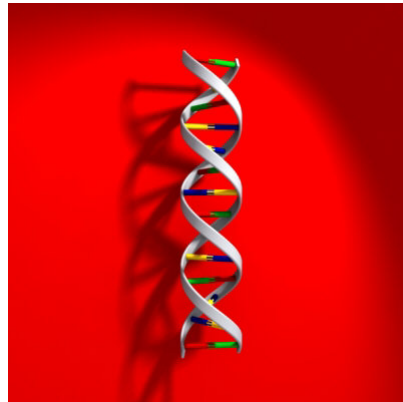
Sustained drug delivery



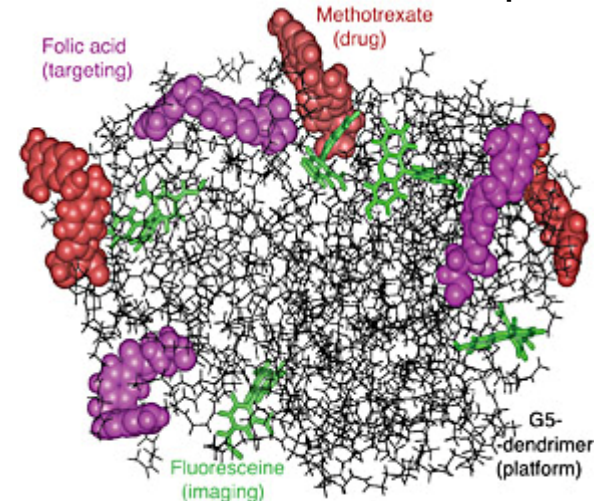
drugs

Cosmetics

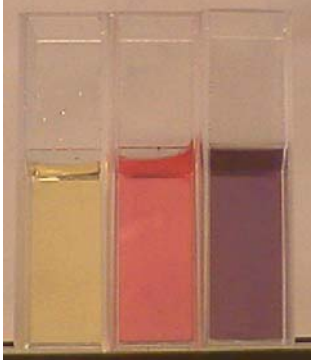
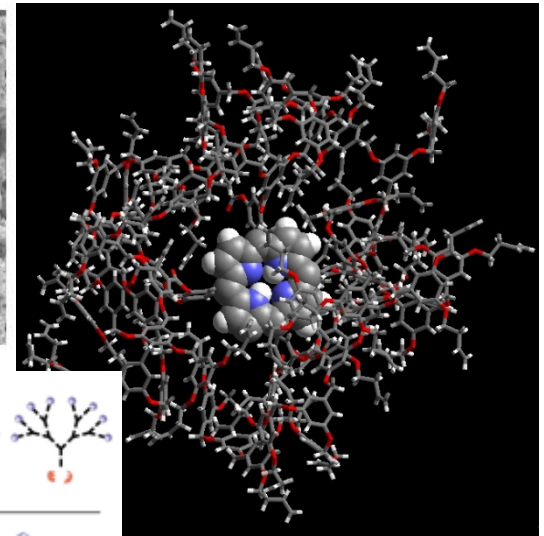
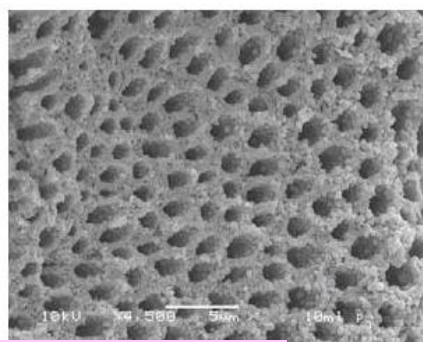
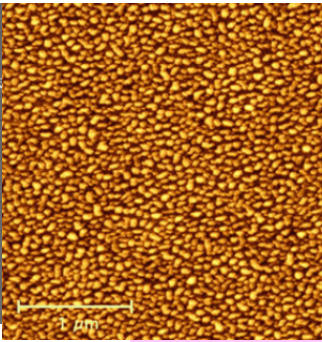
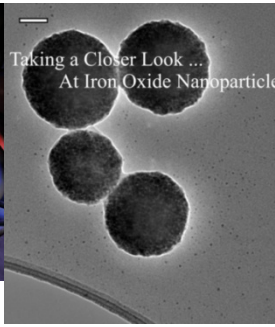
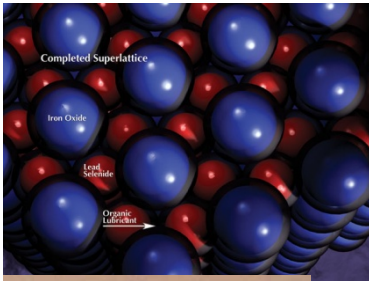
Cancer treatments



superabsorbants



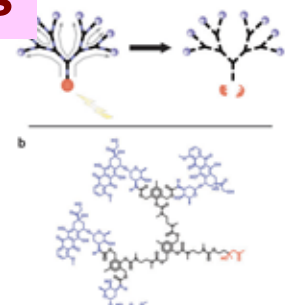
Dendrimers for drug attachments



**Metals**

**Polymer-proteins**

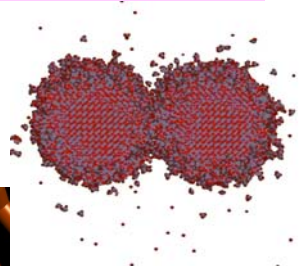
**Materials used**



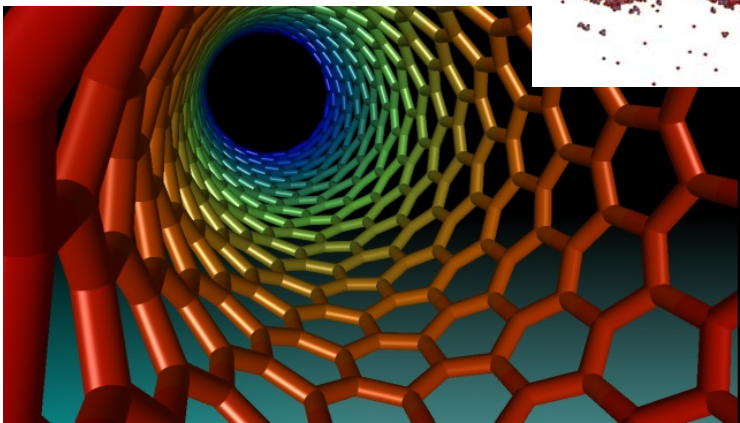
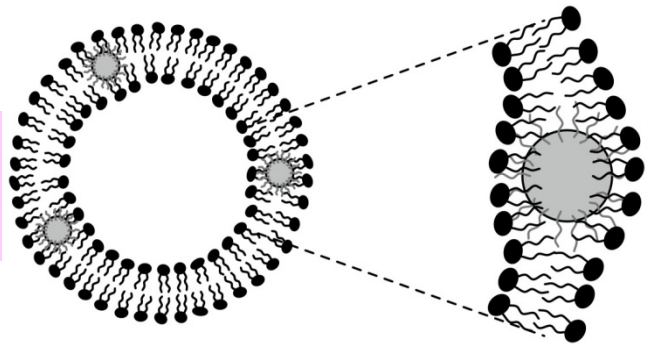
**Dendrimers**



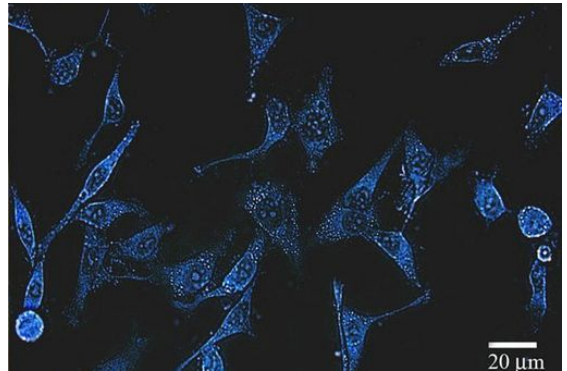
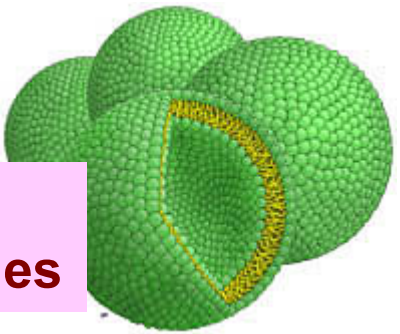
**Ceramics  
Metal-oxides**



**Lipid-based nps**



**CNTs  
fullerenes**





## Therapeutic Benefits:

Solubility (for insoluble drugs)

Carrier for hydrophobic entities

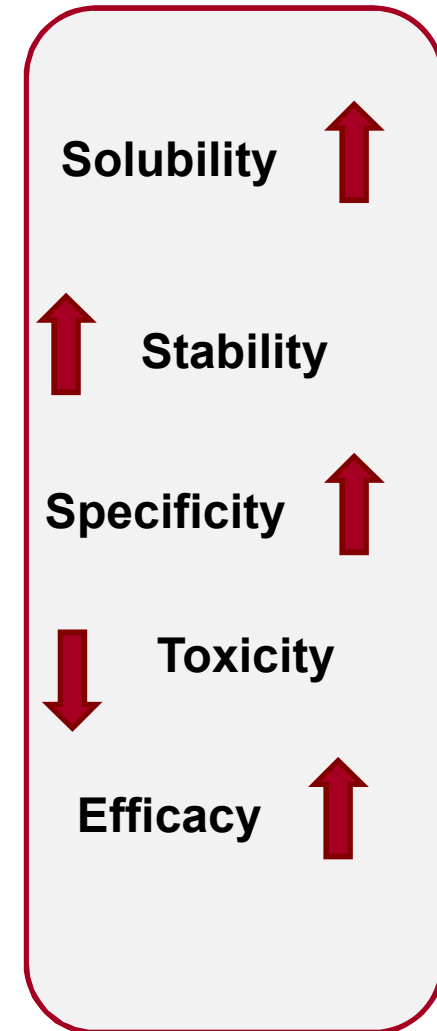
Multifunctional capability

Active and passive targeting

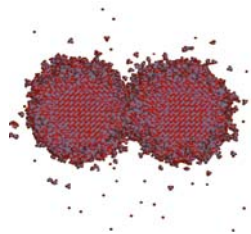
Ligands; size exclusion

Reduced toxicity

## Nanomaterials impart:



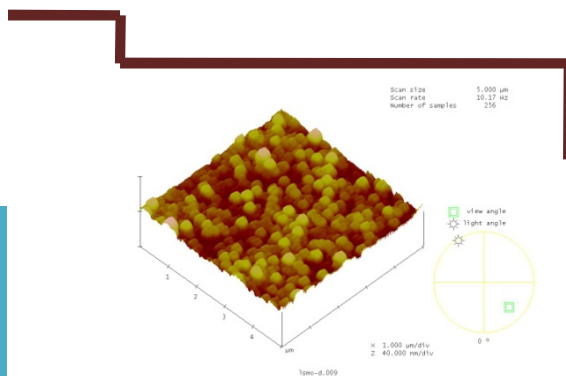
# The Approach



Synthesis:  
Physical properties

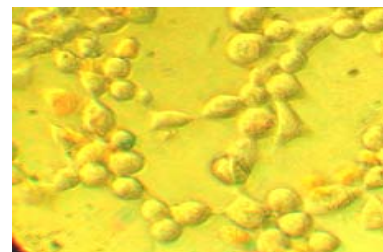
Chemical properties

Quality  
Purity  
Stability



Physical Characterization:

- Size
- Size distribution
- Molecular weight
- Morphology
- Surface area
- Porosity
- Solubility
- Surface charge density
- Purity
- Sterility
- Surface chemistry
- Stability



In Vitro:

- Binding
- Pharmacology
- Blood contact properties
- Cellular uptake
- Cytotoxicity



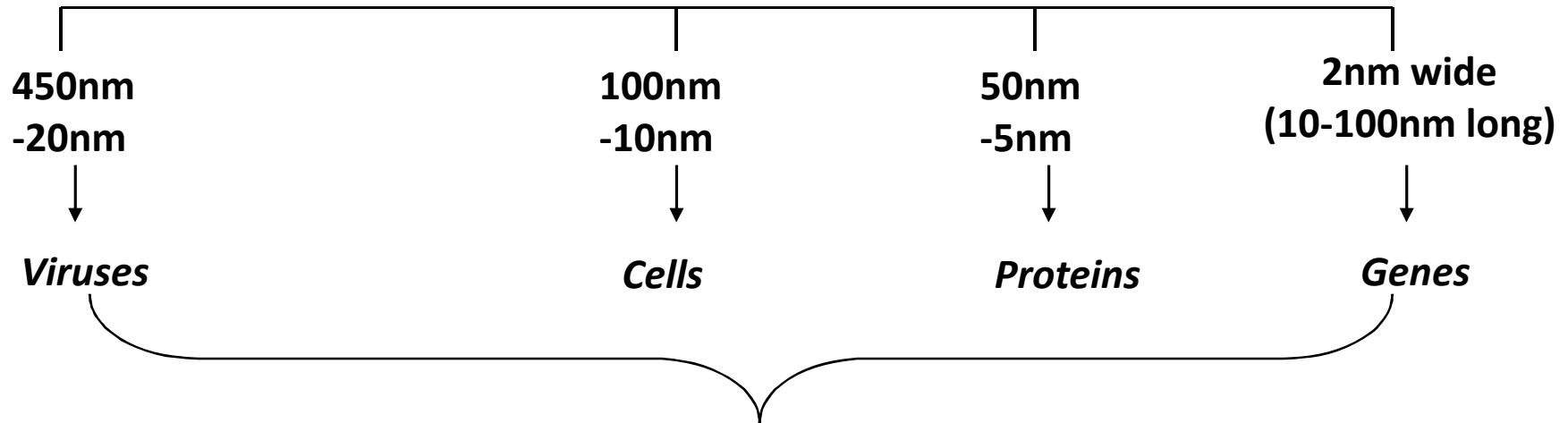
In Vivo:

- Absorption
- Pharmacokinetics
- Serum half-life
- Protein binding
- Tissue distribution
- Metabolism
- Excretion
- Safety



# Magnetic Materials in biomedicine

## *Nanoscale in biological entities*



*Comparable size synthesis  
via soft chemistry routes*



**Magnetic Nanoparticles**

## *Examples of Promising Applications*

**MRI contrast  
agents**

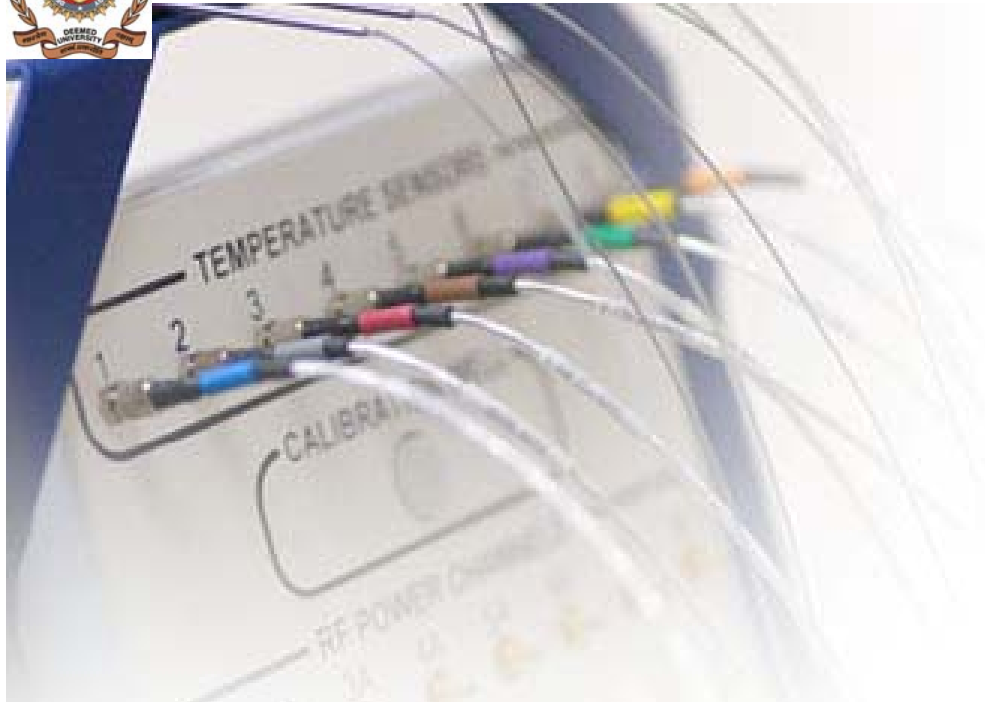
**Magnetic  
separation**

**Magneto-fluids  
in heating  
applications**

**Hyperthermia  
Applications...**



# Magnetic Nanoparticles for Cancer Hyperthermia



## Normal Cells

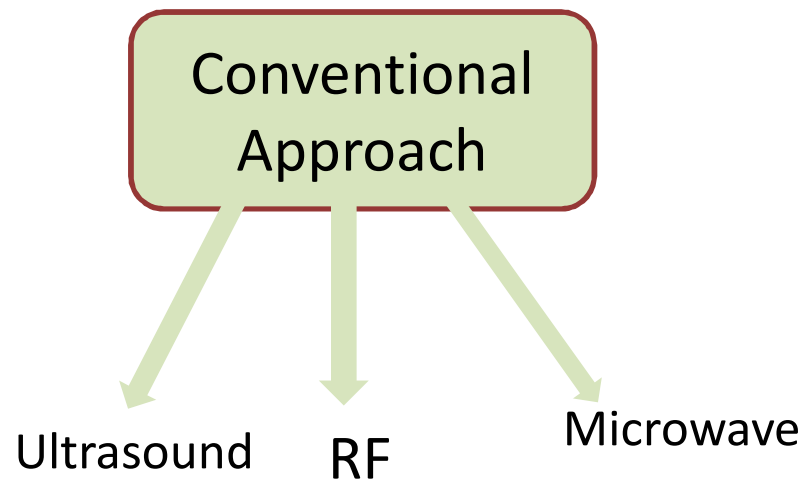
- ❖ Growth is very orderly and precise.
- ❖ Good Cell adhesion
- ❖ Cannot be placed wrongly
- ❖ Pre-programmed to reproduce 50-60 times, maximum
- ❖ **withstand 52°C**

## Cancer Cells

- ❖ Keep on reproducing
- ❖ Do not stick together
- ❖ Do not die if they move to another part of the body
- ❖ Stay immature and continue to multiply
- ❖ **Die at 42-45°C**



# Conventional approach towards Hyperthermia



## Problems:

- Healthy tissue absorption
- Temperatures regulation
- Body penetration issues

## Magnetic Hyperthermia

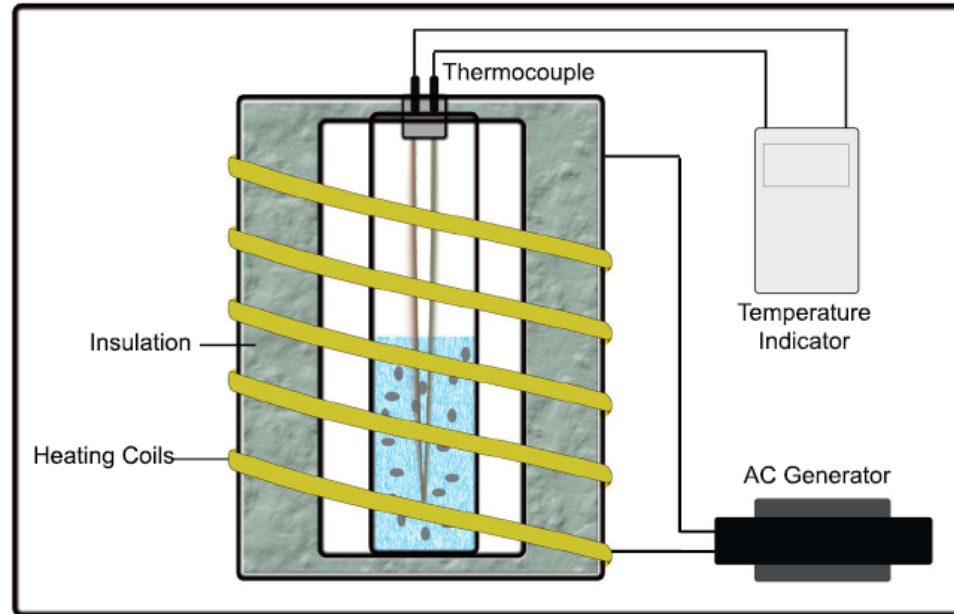
Magnetic particles

Encapsulated ferro/ferri  
Magnetic nanoparticles

*Nanotechnology offers promising capabilities for use of magnetic nanoparticles.*



# Magnetic Nanoparticles for Hyperthermia



**Energy loss in the magnetic material, can be due to:**

a) Magnetic losses through domain wall displacements (in multi-domain particles) called Néel losses; and

b) Energy loss from mechanical rotation of the particles, acting against viscous forces of the liquid medium (Brownian losses).



# Exploring magnetic nanoparticles for Heating Applications





# $Fe_3O_4$ -Citrate-Curcumin: Promising conjugates for superoxide scavenging, tumor suppression and cancer hyperthermia

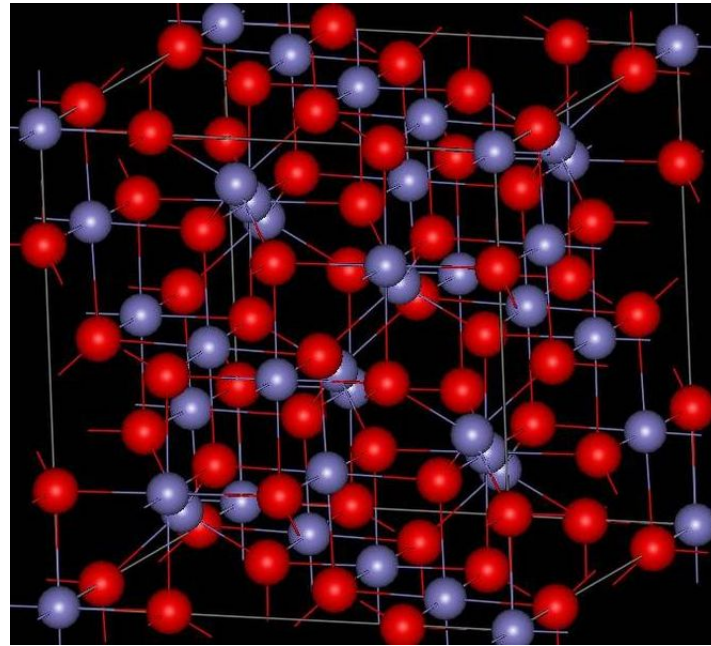
Wani, Rohini et. al. J. NanoBioScience, 2011  
Rohini et.al., Nanotechnology, submitted, 2011

**Also on Poster of Rohini at Nano-BioMed**



# About Magnetites

Spinel  
Ferrimagnetic  
oxide



## Applications mainly harnessed:

Magnetite powder efficiently removes arsenic from water, magnetite as a sorbent

Used for coating industrial water tube steam boilers.

Iron oxides are used as contrast agent in Magnetic Resonance Imaging,

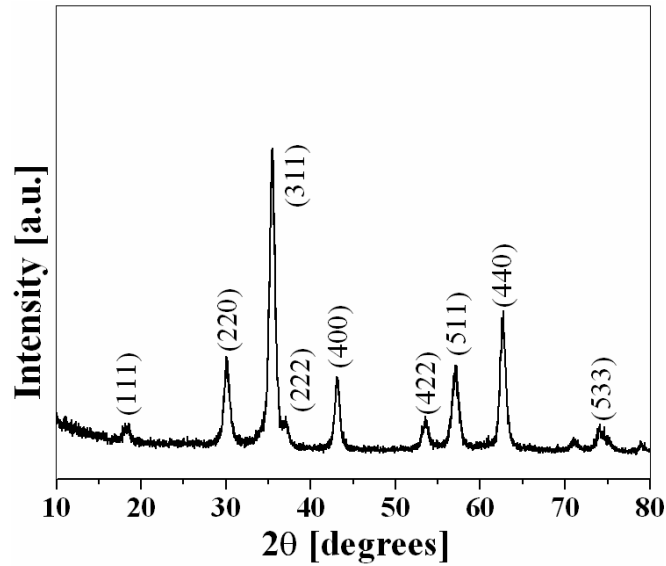
They may also be used in electrochromic paints.

Used as a popular cancer hyperthermia agent



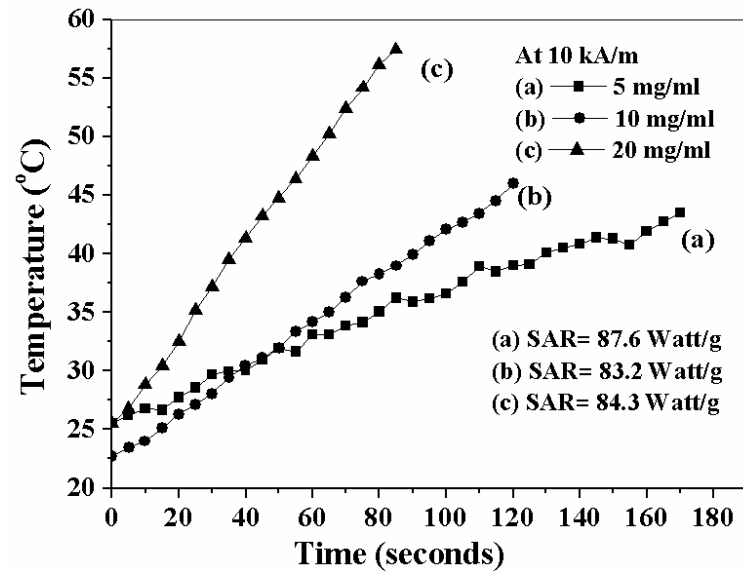
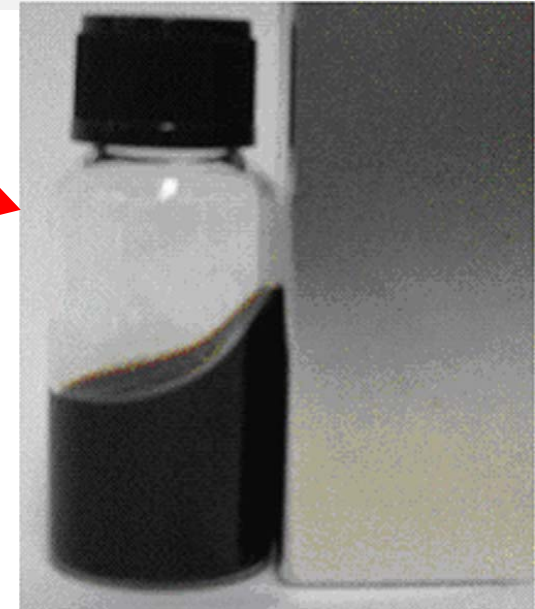
# Background Work

D. Maity et.al. *J.Magn Mag Mater* 321, 2009, 3093



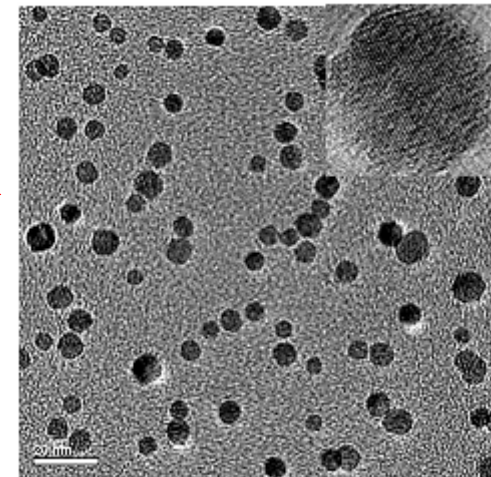
Fe<sub>3</sub>O<sub>4</sub>:TREG system

10 kA/m AC field at 425 kHz frequency



monodispersed faceted crystalline nanoparticles ~10 nm

Good Microwave Absorption



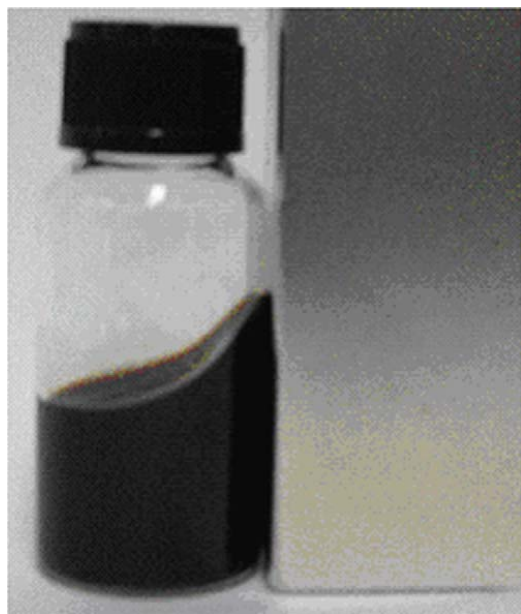


# Experimental

- **Reverse co-precipitation** was used for synthesis of  $\text{Fe}_3\text{O}_4$ .
- Citric acid was introduced as a linker between  $\text{Fe}_3\text{O}_4$  and CU (**Fe-CA-CU**).
- **Physico-chemical characterizations** : XRD, FTIR, TGA, DLS, VSM and TEM
- The **cell viability studies**: MTT dye on MCF7 cell lines.
- **Growth Assays to evaluate anticancer activity** : Colony formation and Soft Agar Assay.
- **Tumor inhibition and suppression** : Potato Assay
- **Antioxidant Activity** : superoxide anion scavenging assay and superoxide radical scavenging assay (riboflavin)



# $\text{Fe}_3\text{O}_4$ Synthesis protocol



J. Giri et al J. Magn Mag Mater 320 (2008) 724

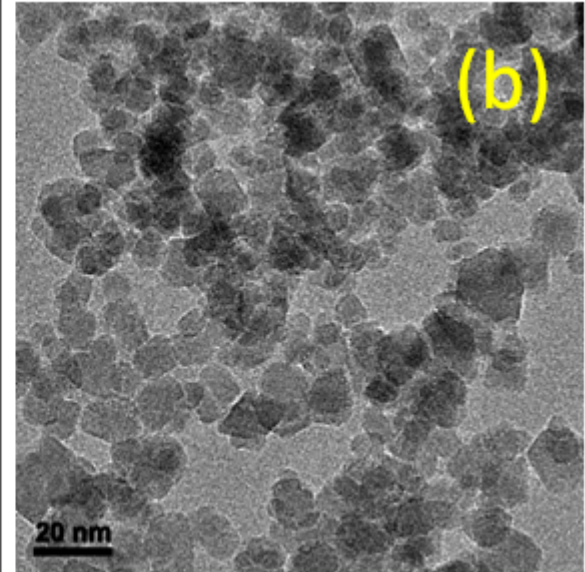
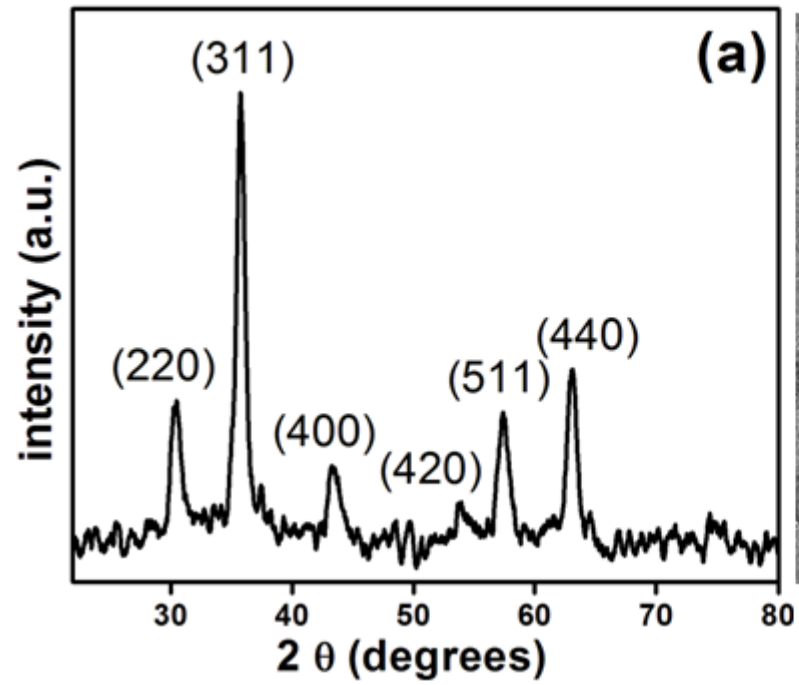
Aqueous solutions Ferrous sulphate and Ferric Nitrate in molar ratio of 1:2

Added in Ammonia and heated to  $80^\circ\text{C}$  under stirring in Ar atm

Cooled and repeated washings to get black slurry

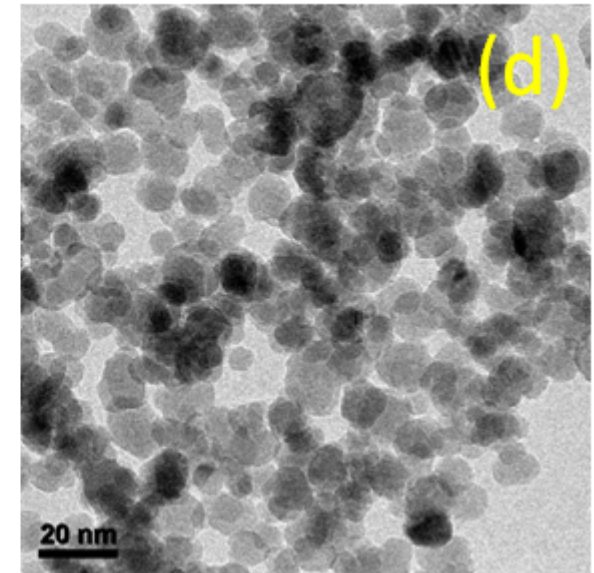
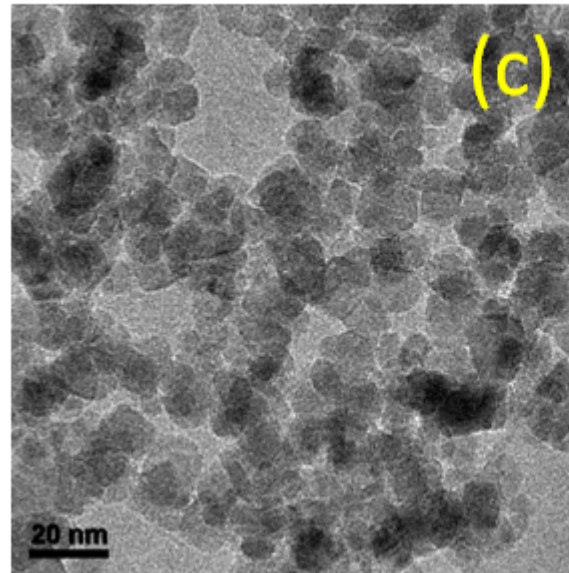
Citric acid (0.5 g/ml) added to  $\text{Fe}_3\text{O}_4$  slurry and heated at  $80^\circ\text{C}$  in normal ambience –constant stirring –cooled and washed.

$\text{Fe}_3\text{O}_4$ :CA



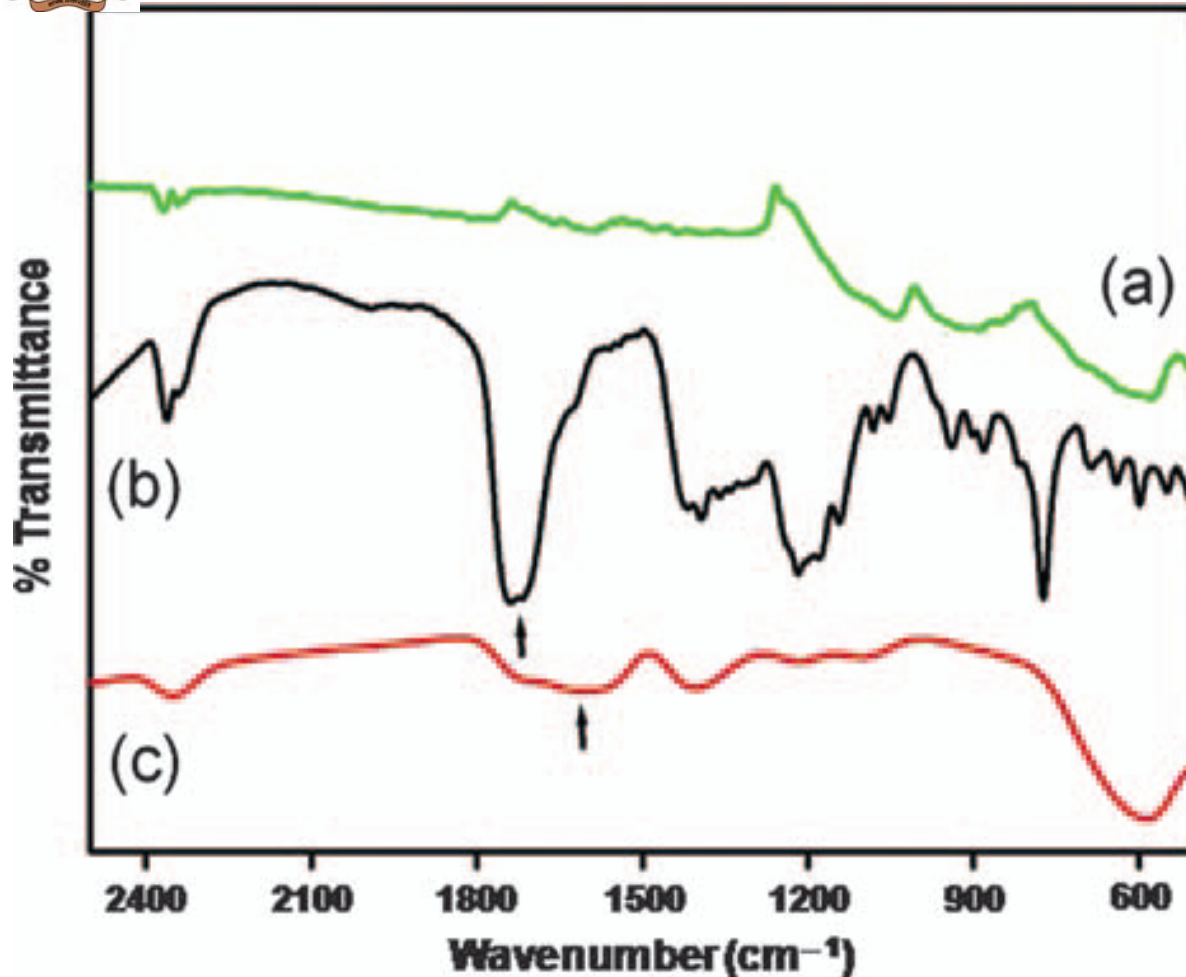
- (b)  $\text{Fe}_3\text{O}_4$
- (c) Fe-CA
- (d) Fe-CA-CU

Cubic Structure, with 12 nm size

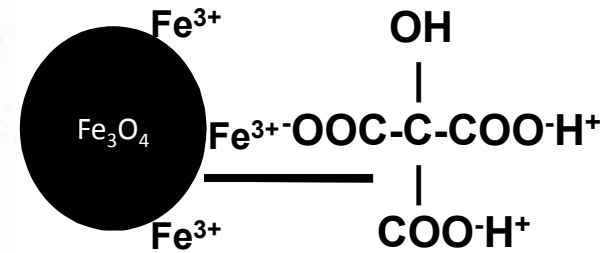




# FTIR to study conjugation of Fe-CA



Shift in C=O signature in CA and presence of COO- signature indicates conjugation of CA with Fe<sub>3</sub>O<sub>4</sub> through carboxylate complex

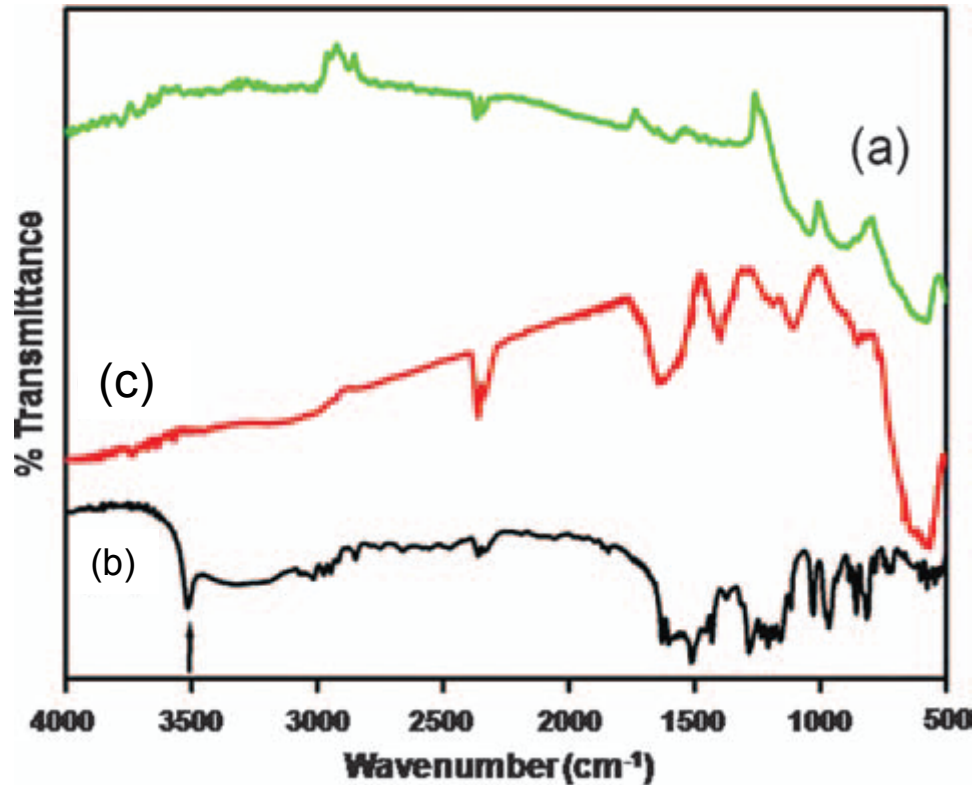


possible Schematic

FTIR of :  
 Fe<sub>3</sub>O<sub>4</sub>(a), CA (b) and CA-Fe(c) nanoparticles.  
 C=O Frequency is recognizable in both CA and Fe-CA



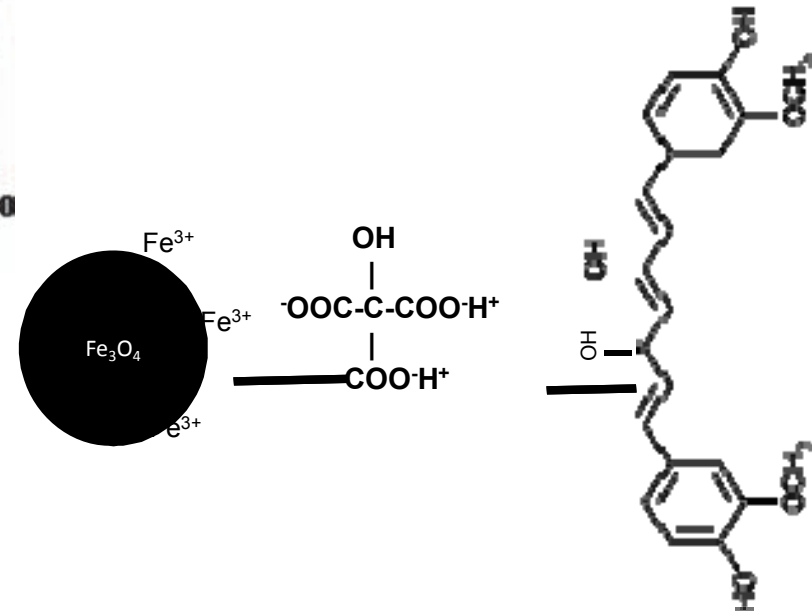
# FTIR to study conjugation of Curcumin with $\text{Fe}_3\text{O}_4$



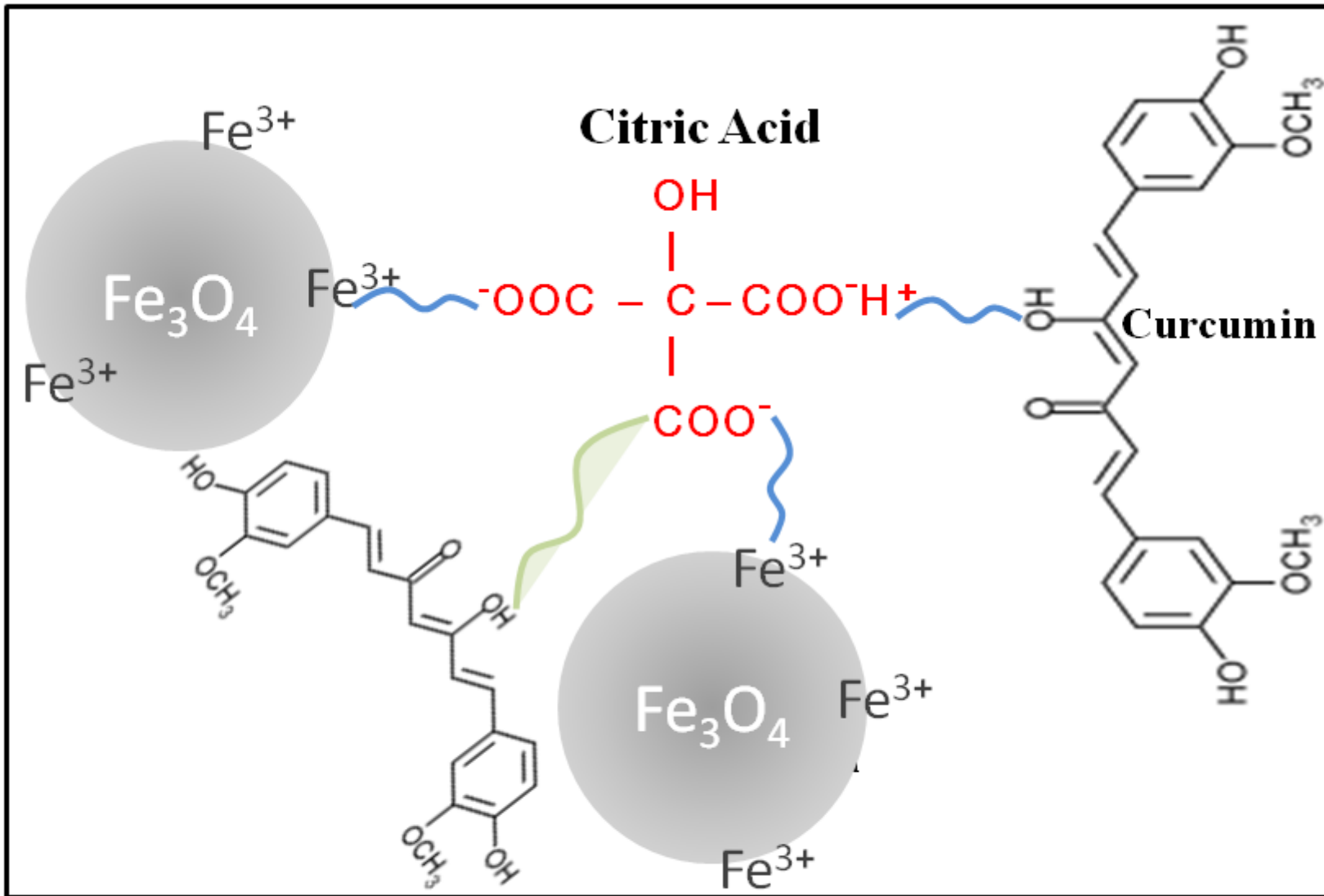
FTIR of :  
 $\text{Fe}_3\text{O}_4$  (a), Fe-CA (b) and Fe-CA-CU (c)

Absence of the broad -OH peak (shown by arrow) in CCF indicates conjugation of CU via one of its -OH bonds

The -COO- signature remains intact, indicating that the interaction between CA and the iron oxide nanoparticle is not disturbed during conjugation of CU to the nanoparticles. This confirms the formation of Fe-CU with CA as a linker between  $\text{Fe}_3\text{O}_4$  and CU



Possible Schematic





## ***Evaluation of Drug Loading in CCF Nanoparticles***

The TGA weight loss was seen at two stages : ~6% (at ~200 C) - be probably due to desorption of CA molecules from the surface of the magnetite nanoparticles with tight binding at the carboxyl site. The second weight ~ 4% loss at a higher temperature (~400 C) that could be due to desorption of CU attached to the magnetic nanoparticles via CA.

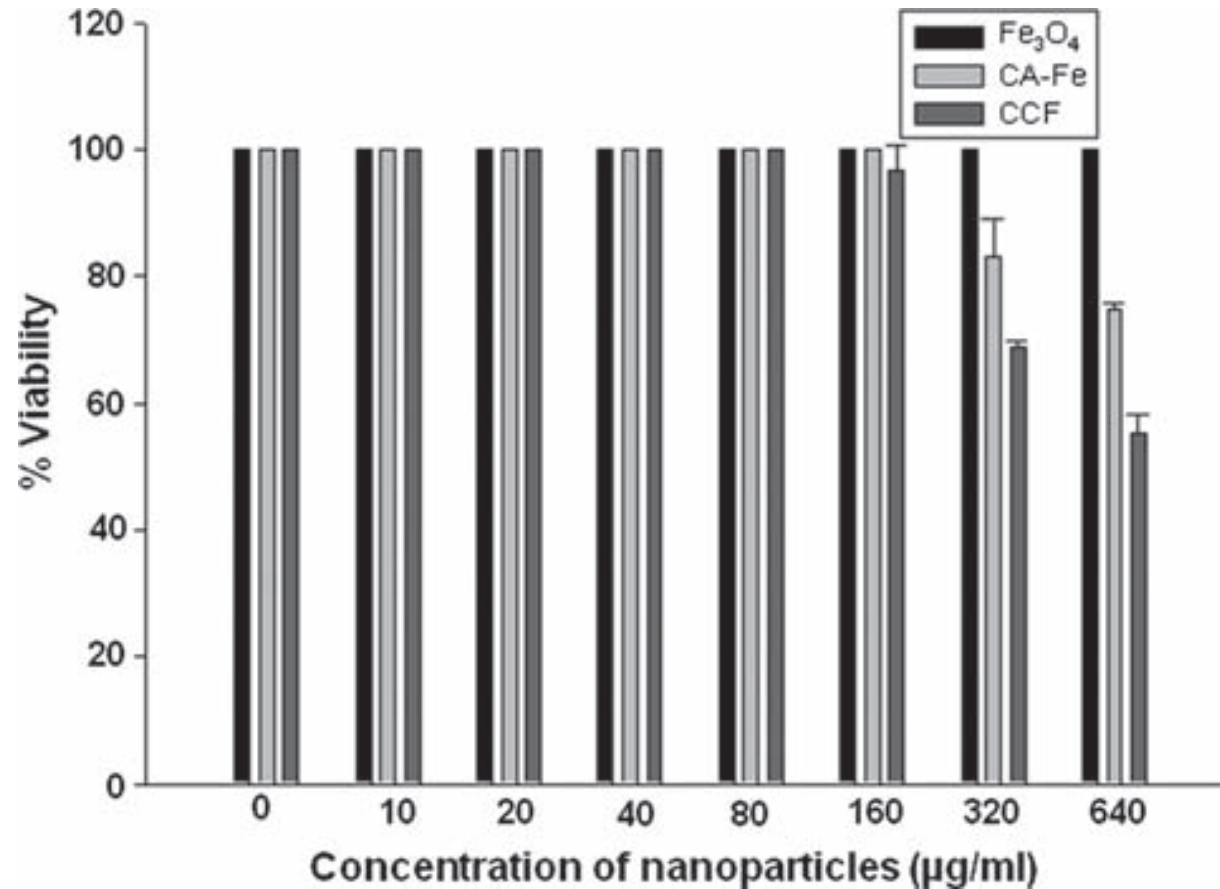
### ***Cell Viability Studies : MTT Assay***

The cell viability study was performed by using MTT dye in breast cancer cell line, MCF7. The cells were grown in DMEM - incubated in a humidified 5% CO<sub>2</sub> atmosphere at 37 C. The cells were seeded at 1×10<sup>5</sup> cells/ml, density in 96-well plates . After 24 h, cells were incubated with fresh medium containing CCF nanoparticles that were added at different concentrations (0 - 640 μg/ml) – incubated overnight at 37 C. The MTT solution (5 μg/ml) was added to each well, and the cells were cultured for another 4 h at 37 C - The intensity of colored formazan derivative was determined by measuring optical density (OD) with the ELISA microplate reader at 570 nm (OD<sub>570</sub>–630 nm).

$$\% \text{Viability} = \frac{\text{Nanoparticle treated cells}}{\text{Control cells}} \times 100$$



## MTT assay



- No cytotoxicity by Fe<sub>3</sub>O<sub>4</sub> and Fe-CA upto 160 µg/ml, indicate that the citric acid attached to the iron oxide nanoparticles did not adversely affect the cells.
- The maximum effect by the Fe-CU at 640 µg/ml proving itself as most potent candidate against MCF7 cells.
- Thus Fe-CU can be a potential candidate for killing the cancer cells, i.e. it can be a healing agent in cancer treatment.



## Colony Formation Assay

The cells - seeded- at density of  $1 \times 10^3$  cells/ml - in a 6-well plate. After 24 h, the cells were dosed with 0, 80 and 160  $\mu\text{g/ml}$  concentration of Fe-CA-CU - Plate was incubated at 37 C in 5%  $\text{CO}_2$  incubator. After one week, the cells were fixed with 4% paraformaldehyde followed by 0.5% crystal violet stain. The colonies were photographed.

## Soft Agar Assay

MCF7 cells ( $5 \times 10^3$  cells/ml) with different concentrations of Fe-CA-CU nanoparticles (40-640  $\mu\text{g/ml}$ ) were mixed at 40 C with 0.35% agarose in culture medium- and gelled at room temperature for 20 min over a previously gelled layer of 0.5% agarose in culture medium in 6-well plates. After incubation for 10 days, colonies were counted directly using an Axiovert 200 M microscope

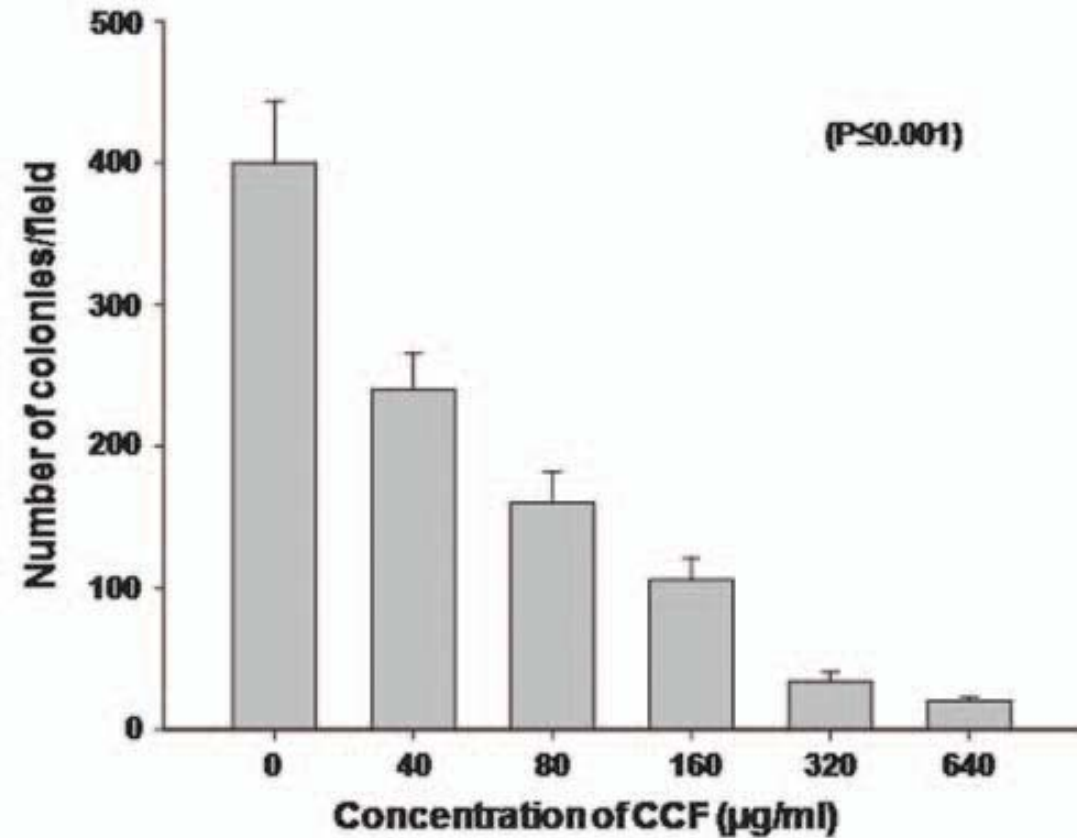
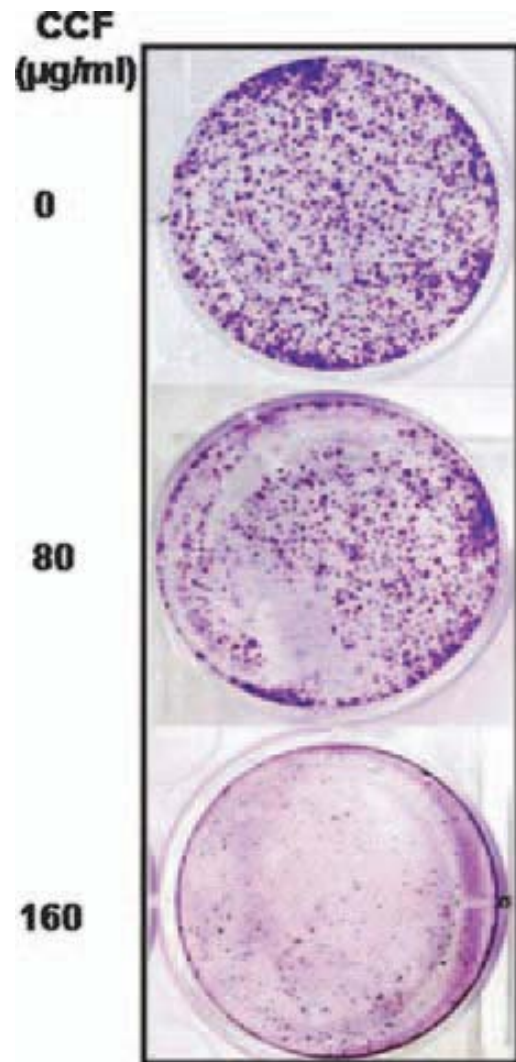
## Determination of In Vitro Uptake of CCF Nanoparticles Into MCF7 Cells

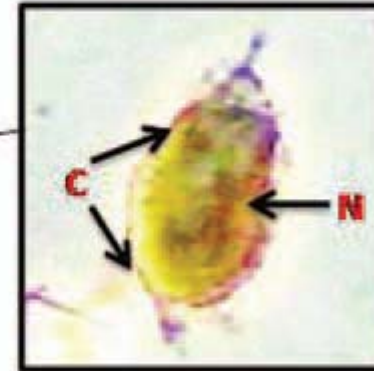
Qualitative evaluation - Fe-CA-CU within the cells was detected by characteristic blue color of Prussian blue.

The cells were seeded - density of  $1 \times 10^5$  cells/ml - After 24 h, the cells were treated with Fe-CA-CU - Post treatment, the cells were fixed in 4% paraformaldehyde for 20 min at room temperature - washed twice in PBS. The coverslips were immersed in a aqueous solns of (20% HCl and 10% potassium ferrocyanide) for 20 min and counter stained using neutral red for 5 min. The stained cells were photographed.



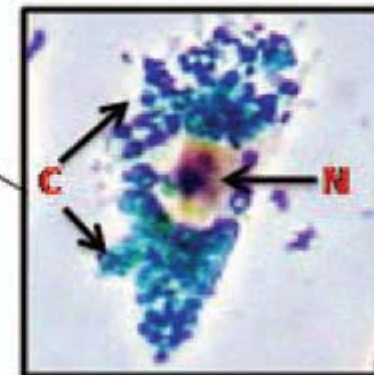
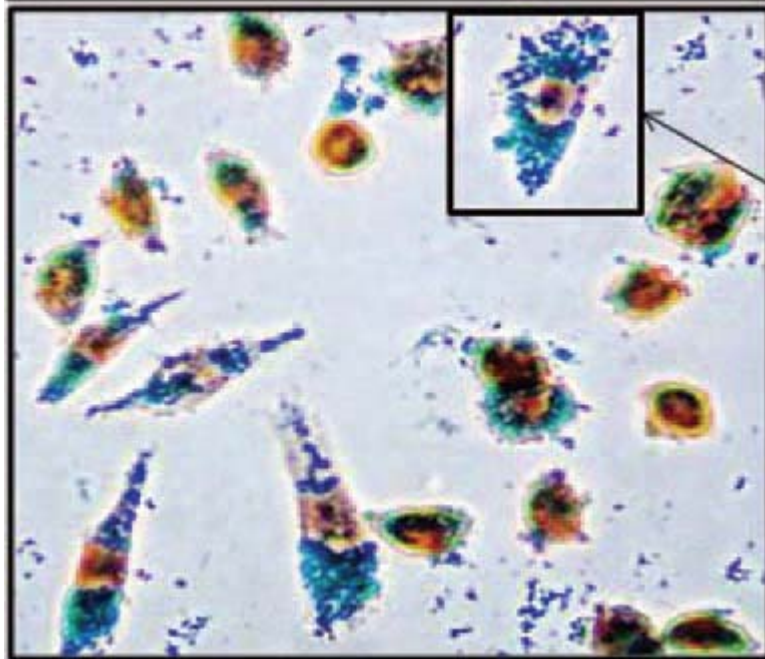
(A) Colony formation assay shows a concentration dependent decrease in the number of MCF7 colonies. (B) Soft agar assay shows a concentration dependent decrease in the number of MCF7 colonies.





*In vitro uptake of nanoparticles into MCF7 cells.*

*(A) Control cells [both cytoplasm (C) and nucleus (N) are orange-red] that are not treated with CCF,*



*(B) Cells treated with 10 g/ml CCF showing uptake of nanoparticles (blue) in cytoplasm.*



## CONCLUSION

Citric acid as a capping agent, wherein it mainly helps in increasing the bioavailability of curcumin.

The present data demonstrates that by using CA in the formation of Fe-CA-CU nanoparticles, the latter showed ferrofluid-like nature in water.

Our cell-based assays showed that the Fe-CA-CU were cytotoxic and could restrict the cell growth in a dose dependent manner thereby confirming that the anticancer property of curcumin was retained in the nanoparticles.

Thus, a novel Fe<sub>3</sub>O<sub>4</sub> capping strategy using citric acid (CA) for better bioavailability of curcumin (CU) was developed that could be used for drug delivery in cancer therapeutics.



# **Fe<sub>3</sub>O<sub>4</sub>-Citrate-Curcumin: for superoxide scavenging, tumor suppression and cancer hyperthermia**

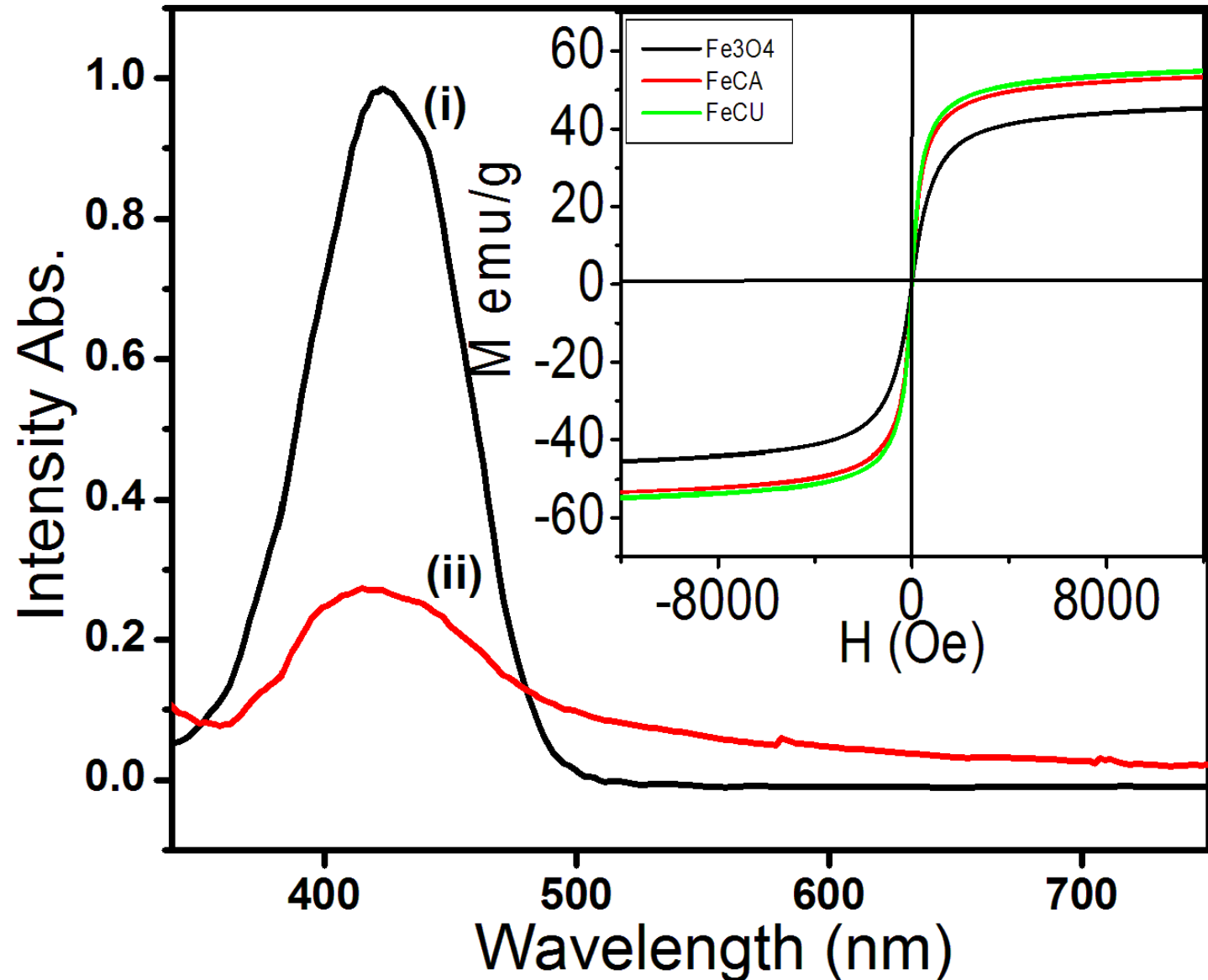
Rohini et.al., Nanotechnology, submitted, 2011



## Curcumin functionality group validation : UV-vis Study

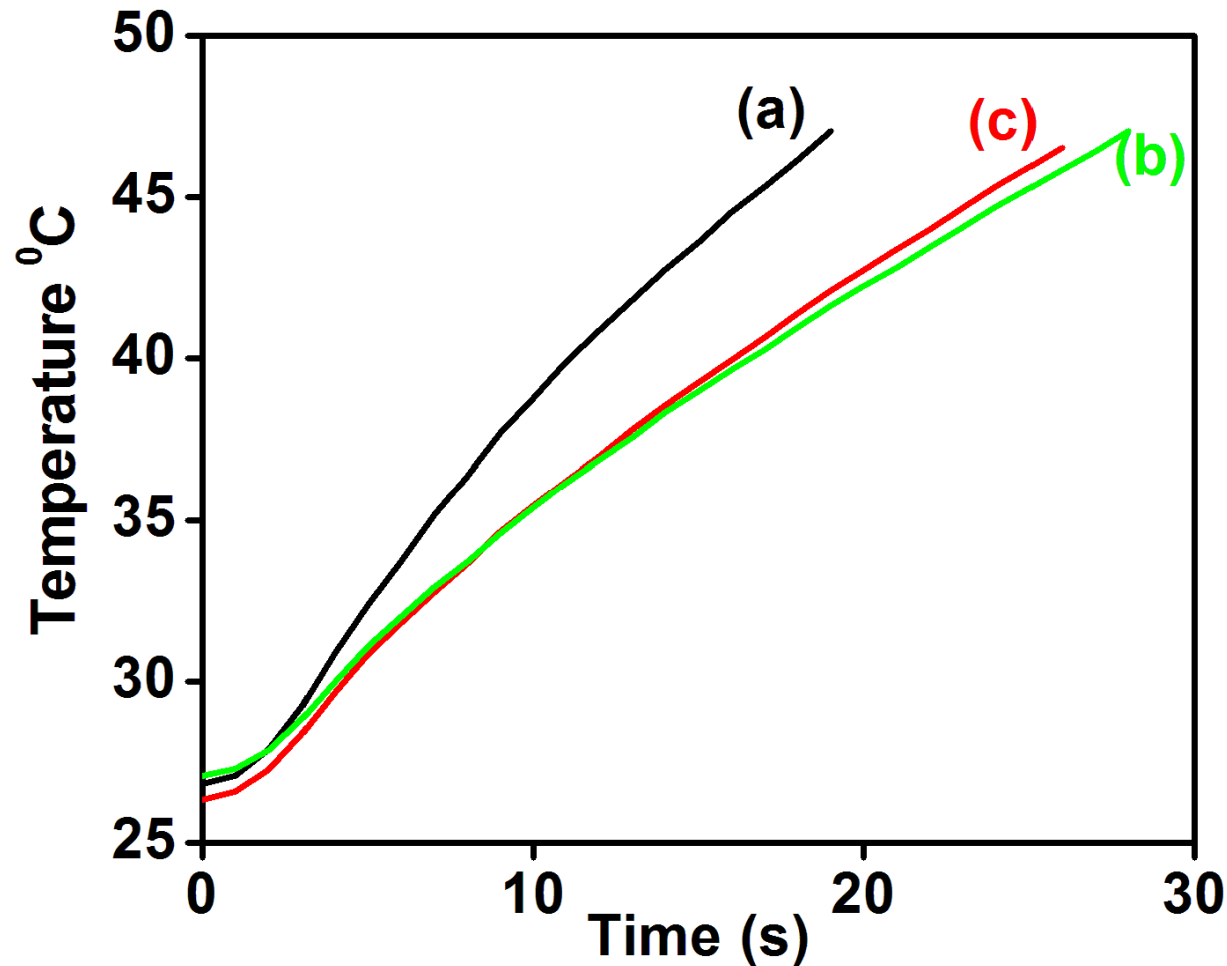
The curcumin's chromophore group seen at 423 nm was intact, ensuring the activity of the molecule.

Magnetisation measurements show good hysteresis curves of  $\text{Fe}_3\text{O}_4$  and Fe-CA-CU, indicating the presence of magnetism after conjugation.





## RF studies : 240 KHz



SAR value has been calculated to be 885 and 539 W/gm of Fe for the sample with iron concentration of 1 and 0.5 mg/ml, respectively.

Probably due to higher RF power.

**10 mg/ml heating rates:**

**$\text{Fe}_3\text{O}_4$  -  $1^\circ\text{C/s}$  , Fe-CA-CU system  $\sim 0.7^\circ\text{C/s}$**

**$\sim 17\text{-}25$  s to reach  $\sim 45^\circ\text{C}$ .**

## Potato bioassay - for evaluation of cancer suppressant and inhibition activity:

Fe-CA-CU, Fe-CA and CU nanoparticles were diluted with sterile distilled water in a microfuge tube.

Sterilized potatoes (*Solanum tuberosum* L., Solanaceae) were cut into 1cm×1cm in size from the center of potato tissue.

Each potato disc was overlaid with 50-70µl of appropriate inoculums.

Following design was used for preparing inoculums: 200µl test nanoparticles (for inhibition studies) + 400µl DDW+400µl *A. tumefaciens*. Potato disks without infection were used as positive control replacing test extract.

After inoculation, Petri dishes were sealed by parafilm and incubated at 27-30°C for 3 weeks.

Tumors were observed on potato discs after 21 days under stereo microscope followed by staining with Lugol's iodine (10% KI and 5% I ) after 30 minutes, where the tumors cells lack starch and each experiment was carried out in triplicate.

For tumor suppression studies, similar procedure was used, however, the test particles (CA, CU, Fe-CA-CU) were subjected to the potato after the tumors were grown and suppression was monitored.



Positive control

Suppression / Inhibition



Negative control

Tumor growth Inhibition



CA



CU



Fe-CA



Fe-CA-CU



Tumor suppression after growth

(I)



**(a)**



**(b)**



**(c)**



**(d)**

**(II)**

Sample	Percent Inhibition
(a) Fresh tumor grown	0
(b) 10 ppm CU & Bacterial culture (control)	95.45
(c) Tumor suppression after 7 days with CU	100
(d) Tumor suppression after 7 days with Fe-CA-CU	88.63

A quantitative estimate, using Potato assay, for tumor suppression showed that while only CU showed 100% suppression in 7 days, it was about 89% by the Fe-CA-CU.

### **Superoxide anion scavenging activity assay:**

Superoxide anions were generated in a non-enzymatic phenazine methosulfate-nicotinamide adenine dinucleotide (PMS-NADH) system through the reaction of PMS, NADH, and oxygen. It was assayed by the reduction of nitroblue tetrazolium (NBT).

In these experiments the superoxide anion was generated in 3 mL of Tris-HCl buffer (100 mM, pH 7.4) containing 0.75 mL of NBT (300  $\mu$ M) solution, 0.75 mL of NADH (936  $\mu$ M) solution and 0.3 mL of different concentrations of the ferrofluid.

The reaction was initiated by adding 0.75 mL of PMS (120  $\mu$ M) to the mixture. After 5 min of incubation at room temperature, the absorbance at 560 nm was measured in spectrophotometer. The super oxide anion scavenging activity was calculated according to the following equation:

$$\% \text{ Inhibition} = [(A_0 - A_1) / A_0 \times 100],$$

where  $A_0$  was the absorbance of the control (blank, without ferrofluid) and  $A_1$  was the absorbance in the presence of the ferrofluid.

### **Super oxide radical scavenging activity:**

The reaction mixture consists of 100  $\mu$ l riboflavin solution (20  $\mu$ g), 200  $\mu$ l EDTA solution (12 mM), 200  $\mu$ l ethanol and 100  $\mu$ l NBT (nitro-blue tetrazolium) solution (0.1 mg) and 100  $\mu$ l of test substance (Fe-CA-CU) at concentrations (300, 600, 900, 1200, 1500  $\mu$ g/ml) were mixed in test tube and reaction mixture was diluted up to 3 ml with phosphate buffer (50 mM). The absorbance of solution was measured at 540 nm using phosphate buffer as blank after illumination for 5 min. A control tube without the test substance but with ethanol served as control.



Compounds	Superoxide anion scavenging assay (in %)	Superoxide radical scavenging assay (riboflavin) (in %)
Fe <sub>3</sub> O <sub>4</sub>	31.81	24.73
Fe-CA	32.33	11.75
Fe-CA-CU	<b><u>40.23</u></b>	<b>100</b>
CA	34.73	24.91
CU	<b><u>38.77 %</u></b>	<b>5.75</b>

Upon subjecting these systems to the superoxide anion scavenging assay and superoxide radical scavenging assay (riboflavin), it was observed that the activity was enhanced in the Fe-CA-CU to 40 % (from 38% in only CU) and 100% (from 5.75% in only CU).



## Conclusions

UV-vis spectroscopy, the curcumin's chromophore group seen at 423 nm was intact, ensuring the activity the molecule.

Magnetisation measurements show good hysteresis curves of  $\text{Fe}_3\text{O}_4$  and Fe-CA-CU, indicating the presence of magnetism after conjugation.

The systems when subjected to radio-frequency fields of 240 KHz, were seen to get heated up, with the  $\text{Fe}_3\text{O}_4$  ( $1^\circ\text{C}/\text{s}$ ) having better slope as compared to the Fe-CA-CU system ( $\sim 0.7^\circ\text{C}/\text{s}$ ) for a sample of concentration 10 mg/ml in average time of  $\sim 17$ -25 s to reach the required hyperthermia threshold temperature of  $\sim 45^\circ\text{C}$ .

A quantitative estimate, using Potato assay, for tumor suppression showed that while only CU showed 100% suppression in 7 days, it was about 89% by the Fe-CA-CU.

Upon subjecting these systems to the superoxide anion scavenging assay and superoxide radical scavenging assay (riboflavin), it was observed that the activity was enhanced in the Fe-CA-CU to 40 % (from 38% in only CU) and 100% (from 5.75% in only CU).

The studies do promise Fe-CA-CU as a cancer hyperthermia-cum-tumor suppressant and antioxidant agent.



# Functionalized Nickel cobaltite nps for drug delivery and cancer hyperthermia

S. Verma et.al. J. Phys. Chem. C 112, 2008, 15106

**Kale et.al., Nanomedicine, accepted, in press, 2011**



# Functionalized Nickel cobaltite nps for drug delivery and cancer hyperthermia

Nearly monodispersed, superparamagnetic nickel cobaltite nanoparticles ( $\text{NiCo}_2\text{O}_4$ ) (NCO) synthesized by combustion method .

Functionalization was done using a biocompatible coat, namely, Mercapto-propionic acid (MPA)

These NCO:MPA nanoparticle showed good radio-frequency absorption, - promising cancer hyperthermia agent.

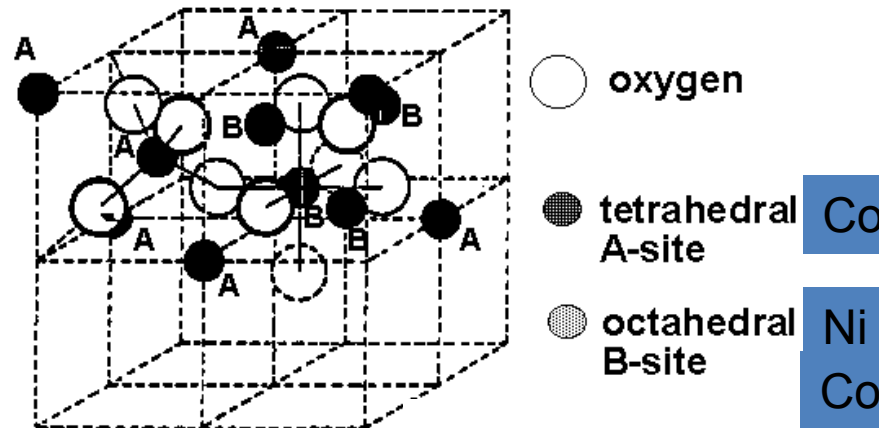
Amino acids, Cysteine and Lysine were conjugated to the NCO:MPA - potential drug-delivery and drug-targeting agent



# About Nickel Cobaltite ( $\text{NiCo}_2\text{O}_4$ )

Spinel  
Multifunctional  
oxide

J. Solid St.Chem. 153, 2000,74



Ni existence of  $\text{Ni}^{2+}$  and  $\text{Ni}^{3+}$ .  
Co is present as  $\text{Co}^{2+}$  and  $\text{Co}^{3+}$

Applications mainly harnessed:  
(TCO - transmissivity from visible wavelength -  $12\mu\text{m}$  IR region)

Electrodes for solar cell applications  
Electro synthesis  
Flat panels displays  
sensors  
n-type semiconductors

The distribution of the cations is a matter of controversy.

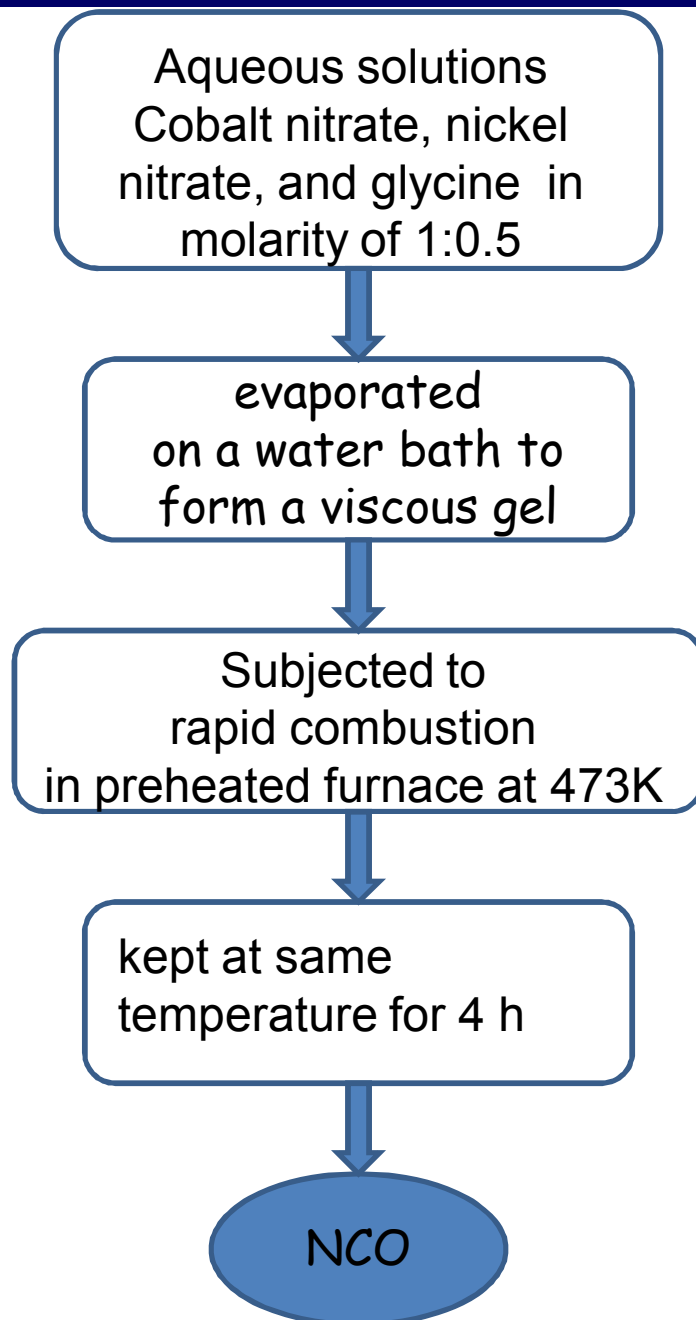
Due to the instability of NCO in air at a temperature  $> 673$  K, -- need for low temperature synthesis

Also in magneto-fluid applications ...



# NCO Synthesis protocol

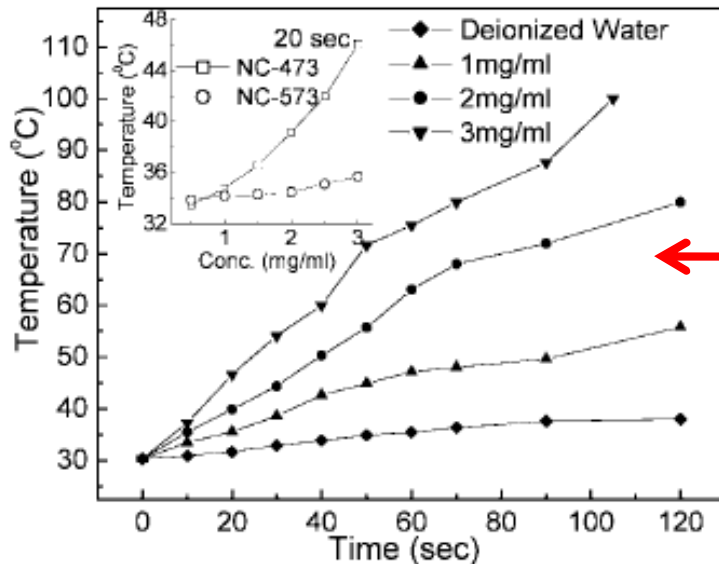
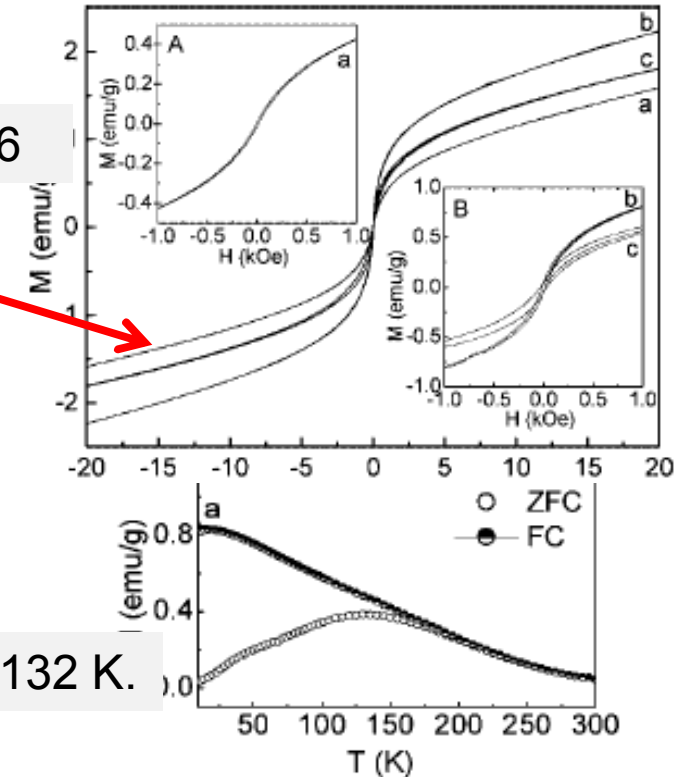
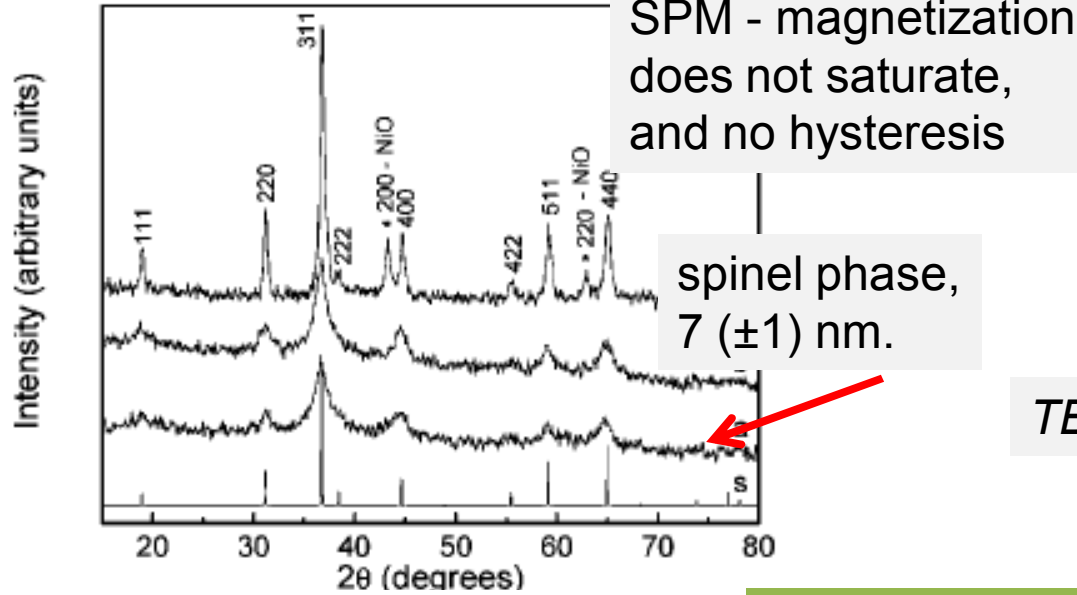
S. Verma et.al.  
J. Phys. Chem. C  
112, 2008, 15106





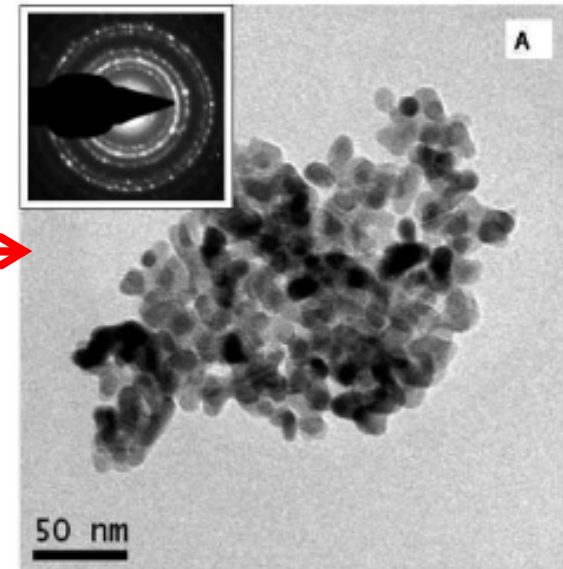
# Background Work

S. Verma et.al. J. Phys. Chem. C 112, 2008, 15106



monodispersed faceted crystalline nanoparticles

Good Microwave Absorption





# NCO-MPA Synthesis protocol

2 mM MPA + 10 mL  
methanol

Sonicated for 10 min

20 mL of this solution,  
added to 30 mL water

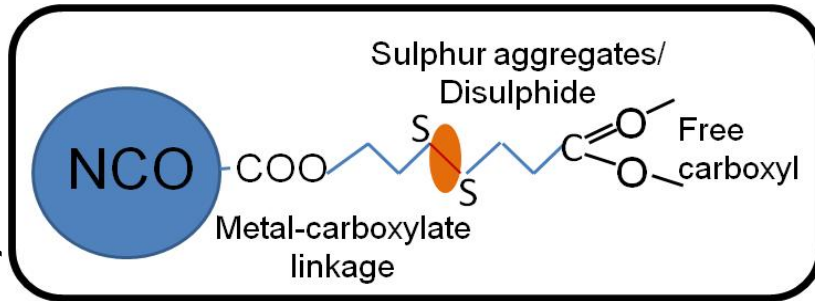
Kept at 80°C for stabilization  
and later cooled

NCO:MPA precipitated using  
acetone-based precipitation

Repeated to  
remove excess MPA

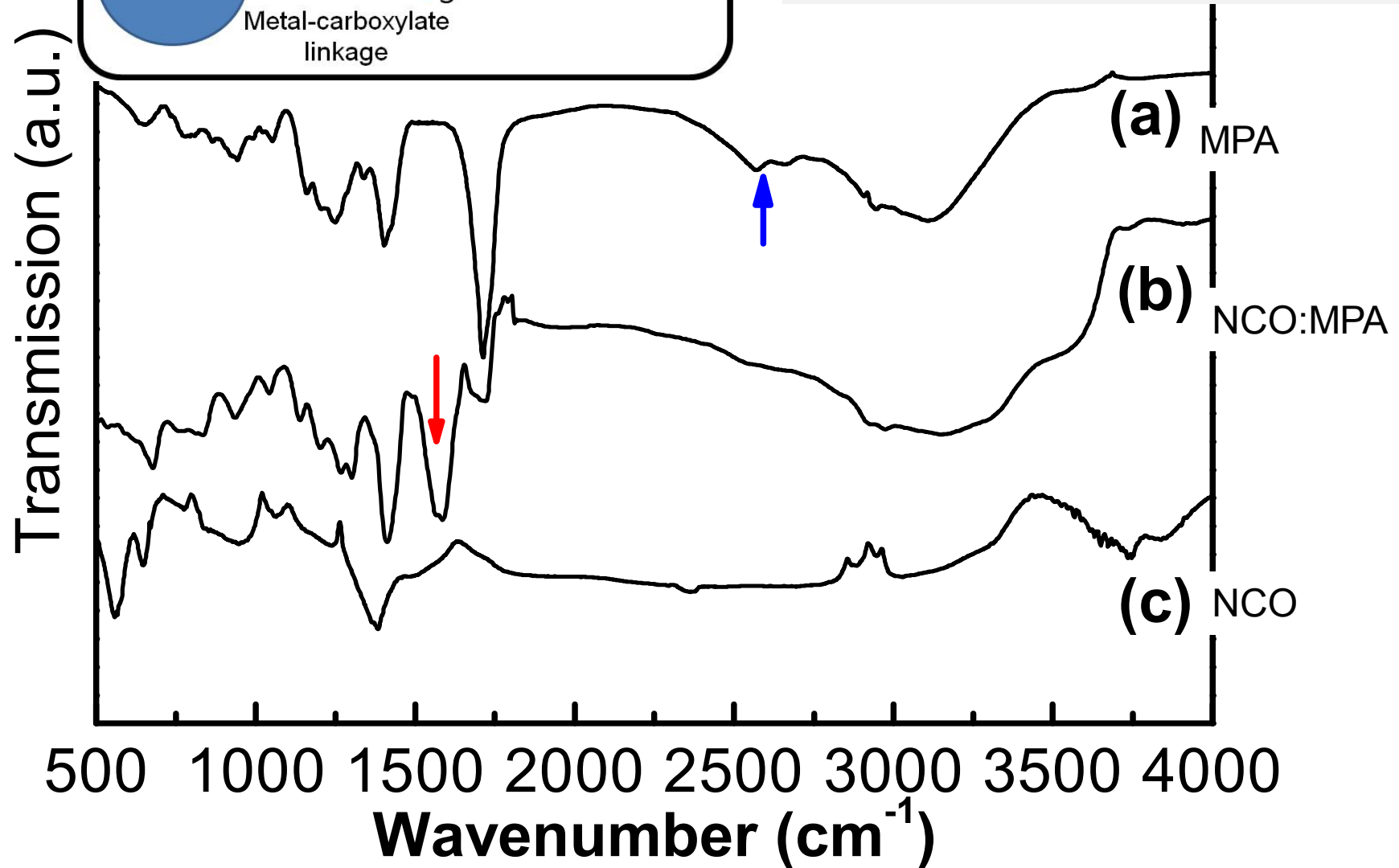
NCO:MPA

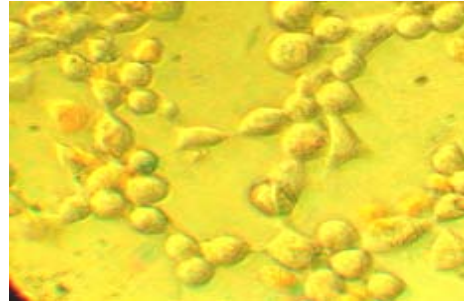




Free carboxyl :  $\sim 1700 \text{ cm}^{-1}$   
Metal oxide-carboxyl group vibrations  $\sim 1600 \text{ cm}^{-1}$

Environ. Sc. Technol **2007**, 41, 5114

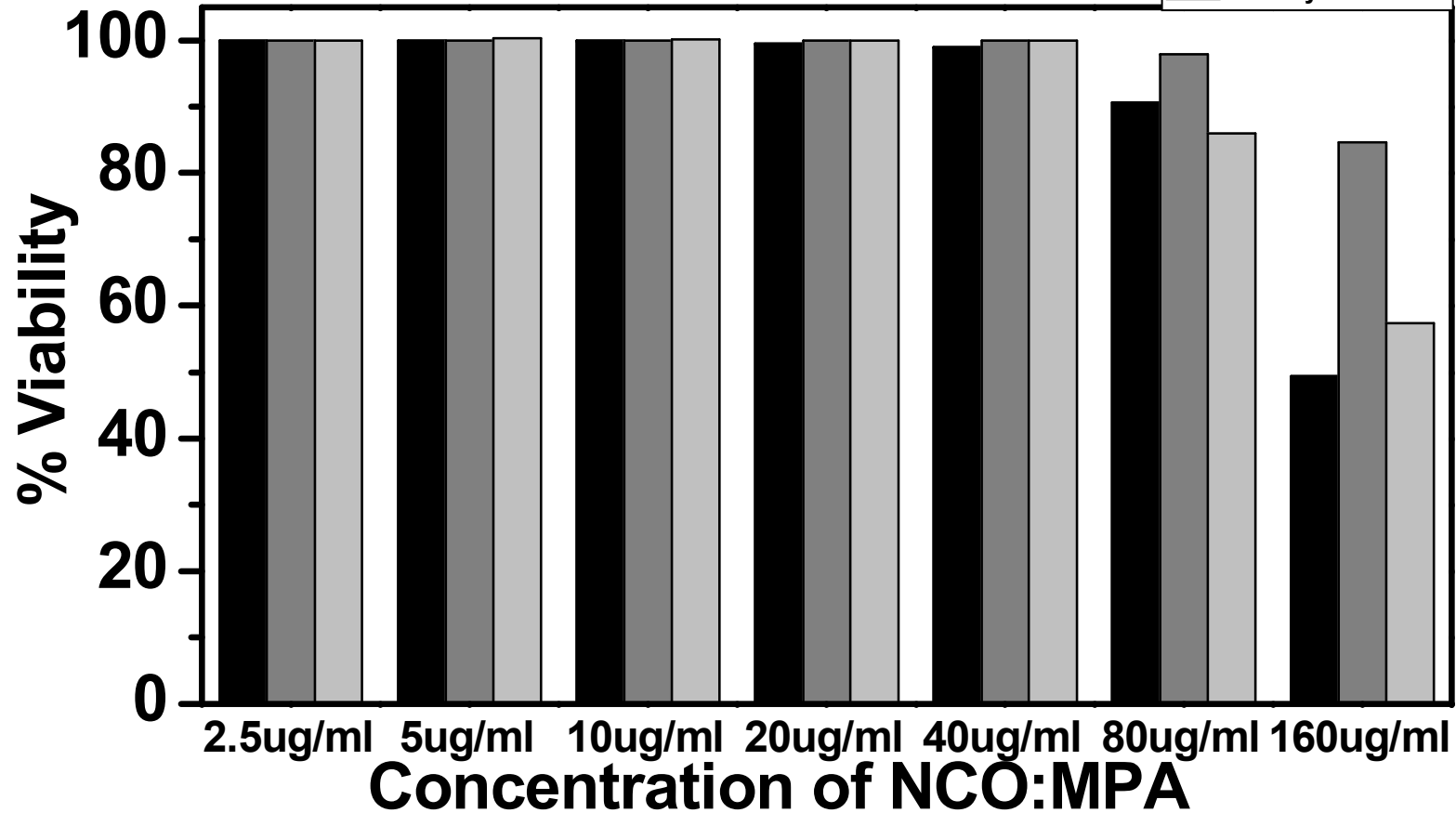




# Cytotoxicity Tests

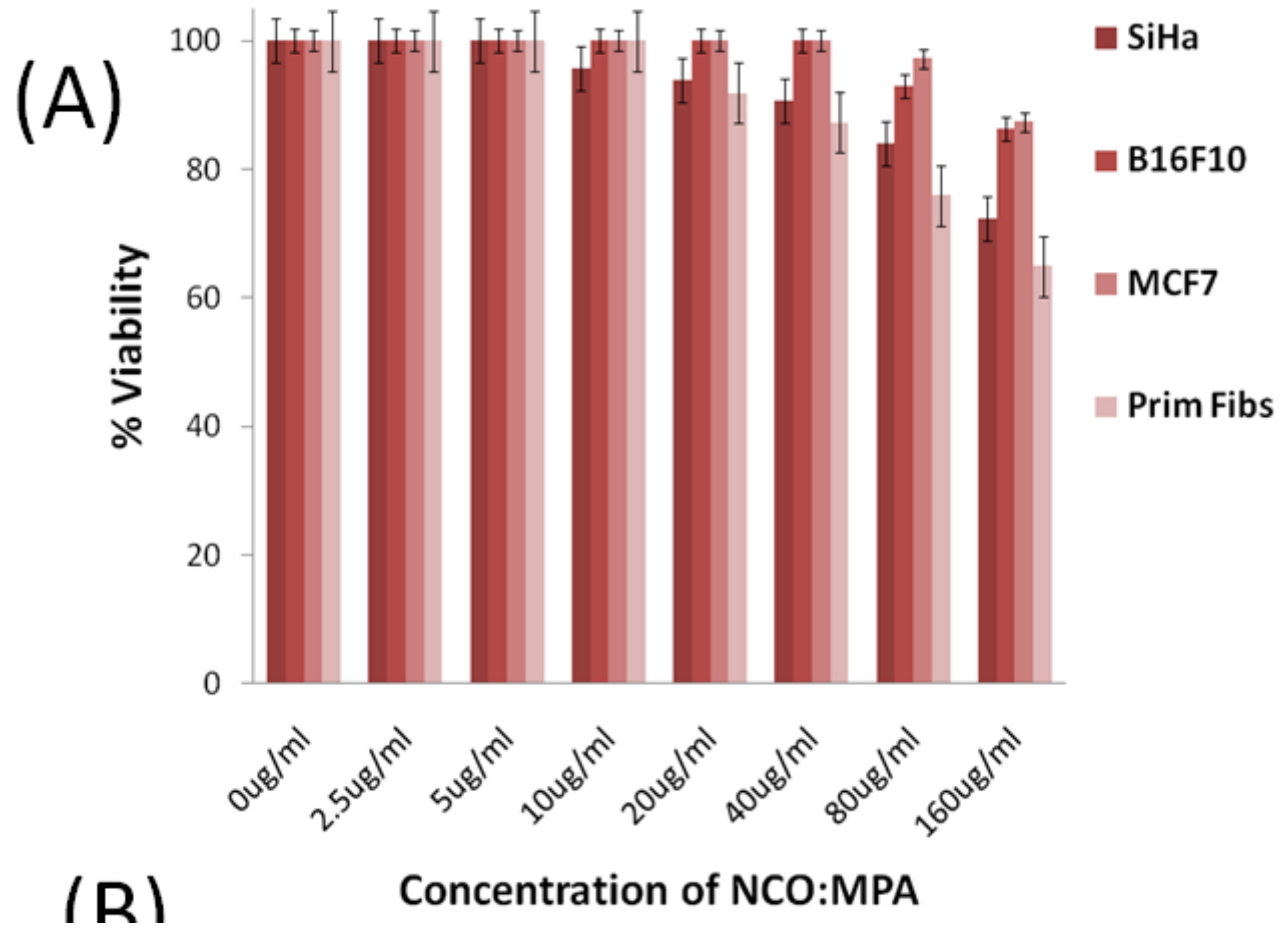
Cervical  
Skin cell lines

■ SiHa  
■ B16F10  
■ Primary Fibroblast



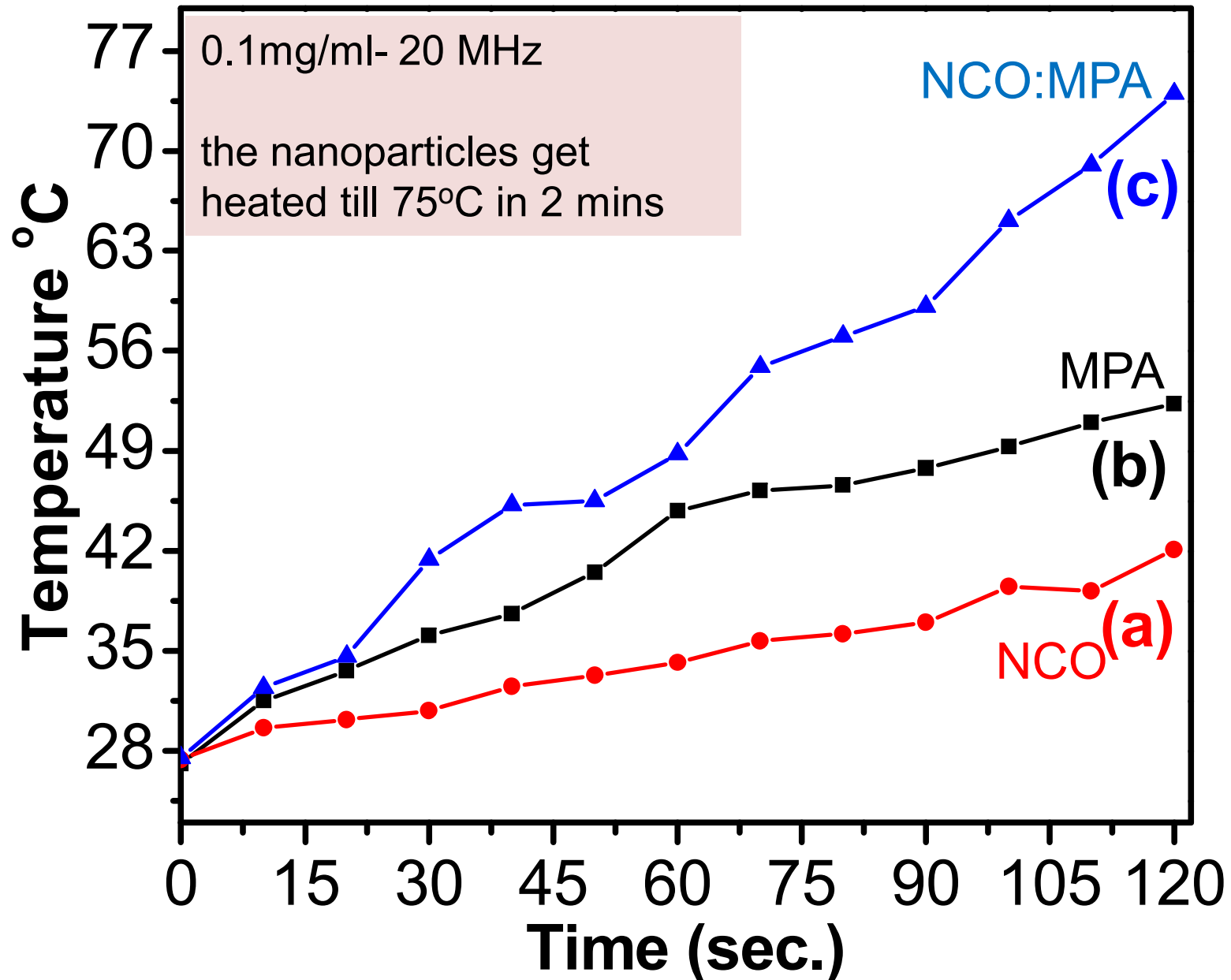
Leaching studies :

Negligible leaching of Co or Ni from the samples - NCO appears to be a stable system in water: as seen using AAS.



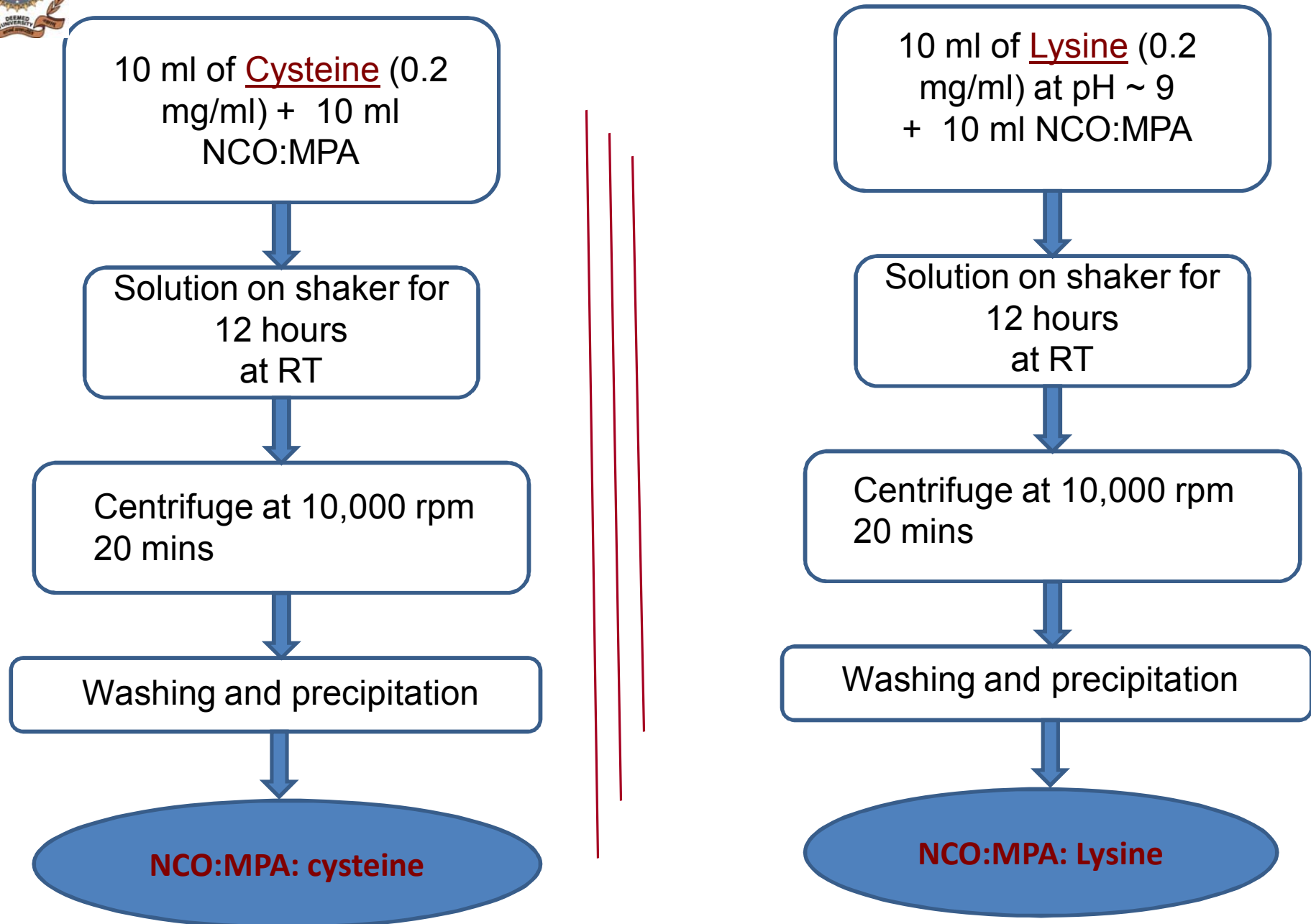


# RF Absorption

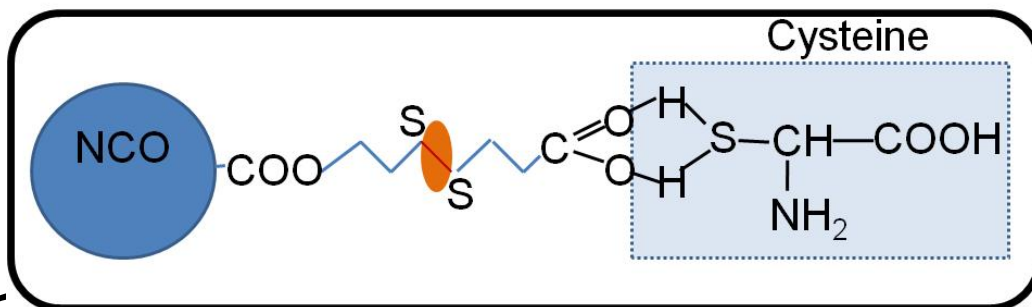




## With amino-acids conjugation ..



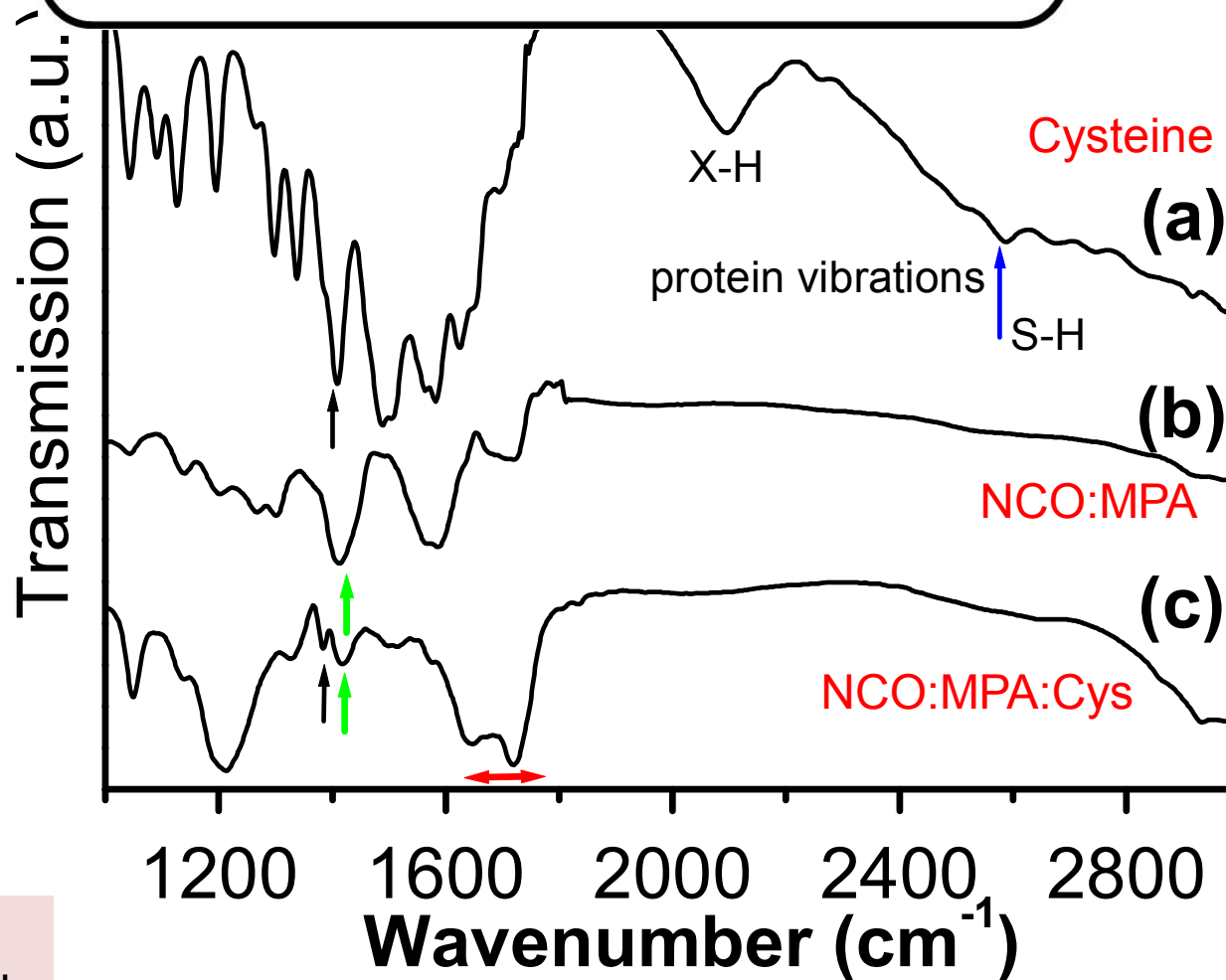
**NCO:MPA:  
cysteine**



1480 – 1760  $\text{cm}^{-1}$  in b) -  
shifted (red arrow)

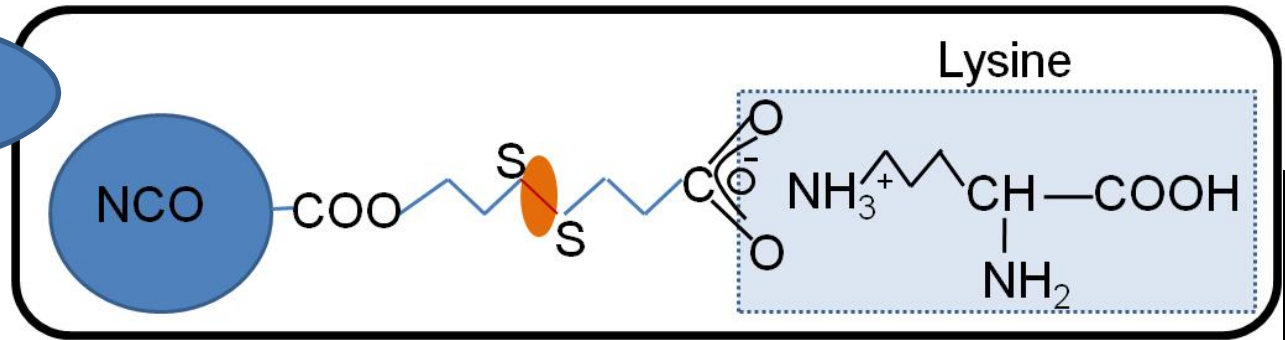
Blue arrows - S-H  
stretch of cysteine-  
suppressed in adduct

black arrows -  
signatures of cysteine



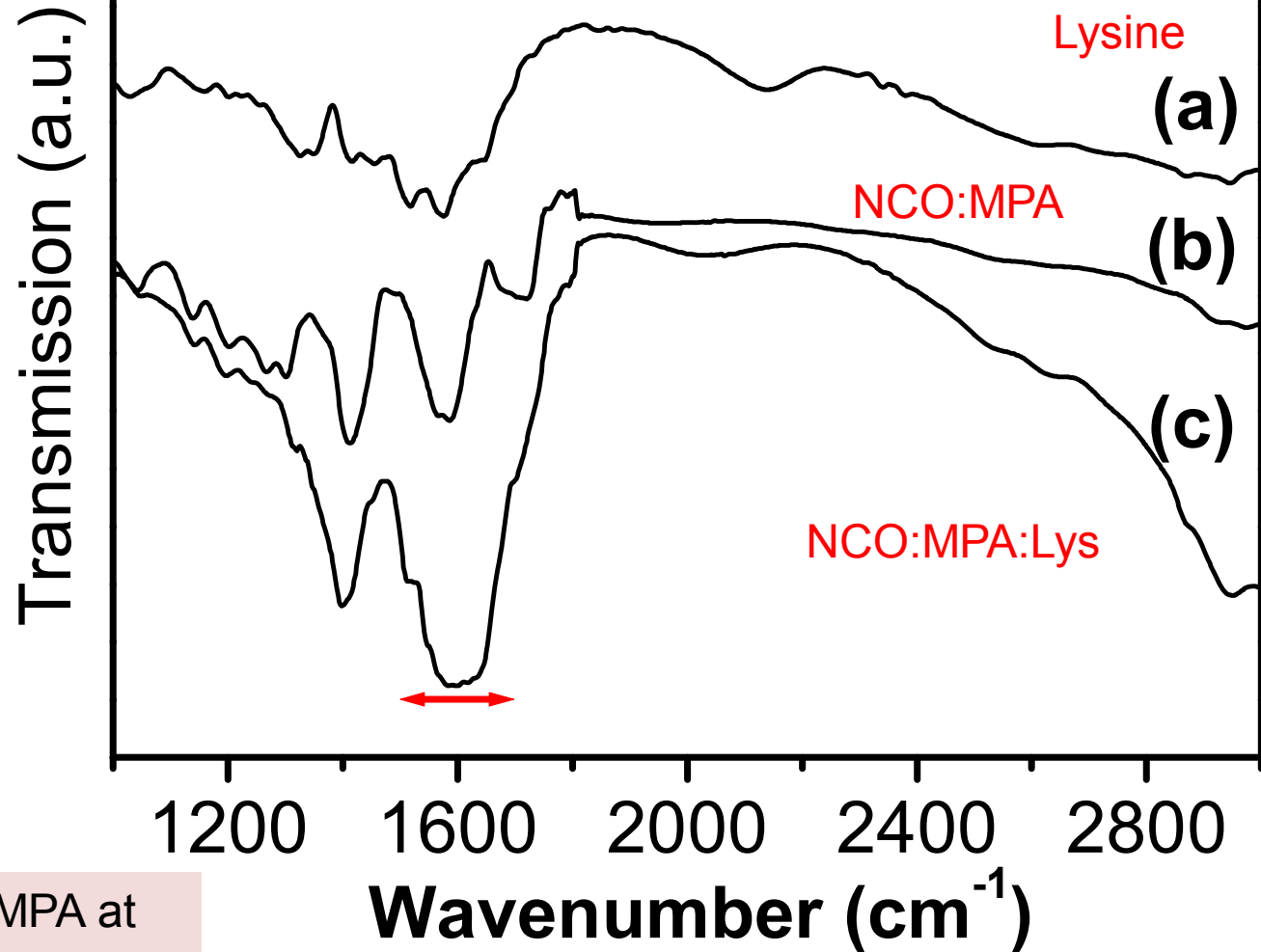
Cysteine conjugated to  
MPA at - free carboxyl end  
via formation of a dimer

**NCO:MPA: Lysine**



No shift in this system.

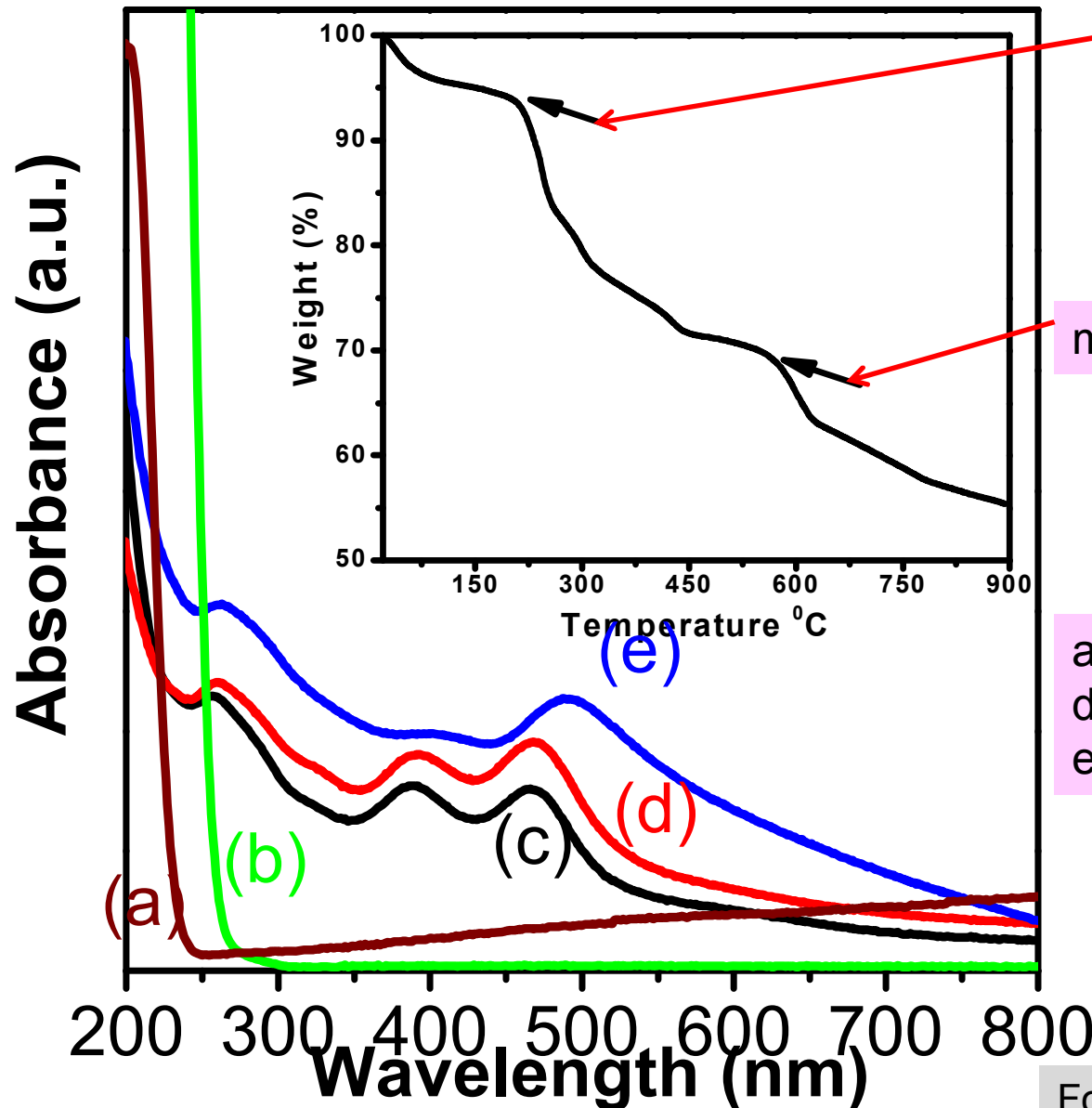
overall increase in the signature intensity in the range of 1480 – 1680 cm<sup>-1</sup> - which, for lysine, is also assigned to NH group.



Lysine -conjugated to MPA at free carboxyl end via an electrostatic interaction.

UV-vis for NCO:MPA sample:

TGA for NCO:MPA sample:

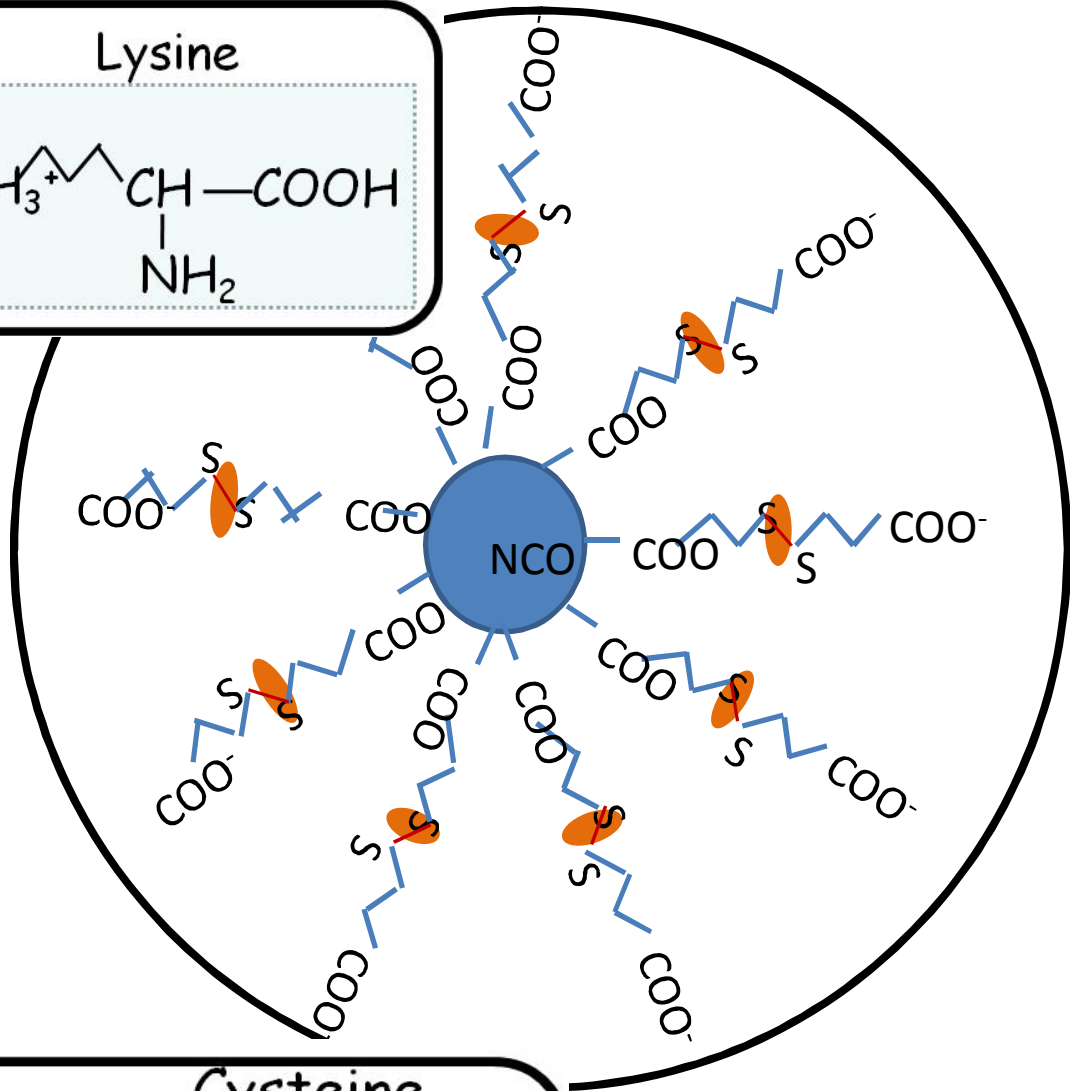
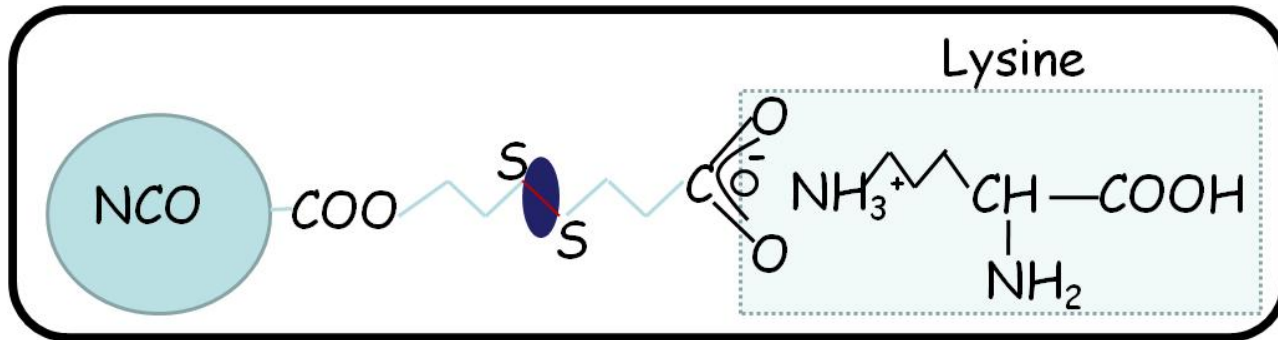


decomposition of sulphides and carboxylates

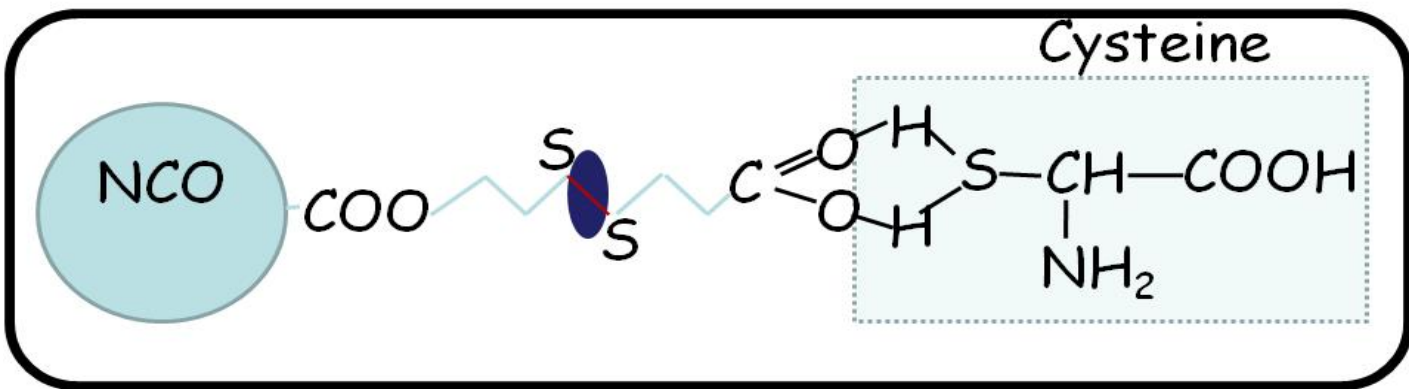
metal-carboxylates

a) NCO, b) MPA, c) NCO:MPA, d) NCO:MPA:cysteine, e) NCO:MPA lysine.

Food Hydrocoll **2003**, 17, 469.  
J. Synch. Radiat. **2009**, 16, 163.



*The Bio-Chemistry ...  
Extremely encouraging for  
Drug-Delivery Applications  
Along with hyperthermia!*





# Conclusions

Nearly monodispersed, superparamagnetic nickel cobaltite nanoparticles ( $\text{NiCo}_2\text{O}_4$ ) (NCO) synthesized by combustion method . Functionalization was done using a biocompatible coat, namely, Mercapto-propionic acid (MPA)

The cytotoxicity studies on NCO:MPA nanoparticles show cell viability of  $\sim 100\%$  up to a dosage of 40mg/ml on SiHa and B16F10 cell lines as well as on mouse primary fibroblasts.

Negligible leaching ( $< 5$  ppm) of ionic Co or Ni was observed into the delivery medium, indicating stability of these nanoparticles.

On subjecting the NCO:MPA nanoparticle dispersion (0.1mg/ml) to a radio-frequency absorption of 20 MHz, the nanoparticles get heated, suggesting it to be a promising cancer hyperthermia agent.

Further two different amino acids, namely Cysteine and Lysine were conjugated to the NCO:MPA system to evaluate the potential of MPA:NCO nanoparticles as possible drug-delivery as well as drug-targeting agent



## Transition temperature-tuned Manganite nanoparticles conjugated with proteins and biopolymers for:

- Cancer hyperthermia
- Drug delivery

**Journal of Biomedical Nanotechnology, 2007**

**Ceramics International, 2007**

**Nanomedicine, 2007**

**Nanotechnology, 2008**



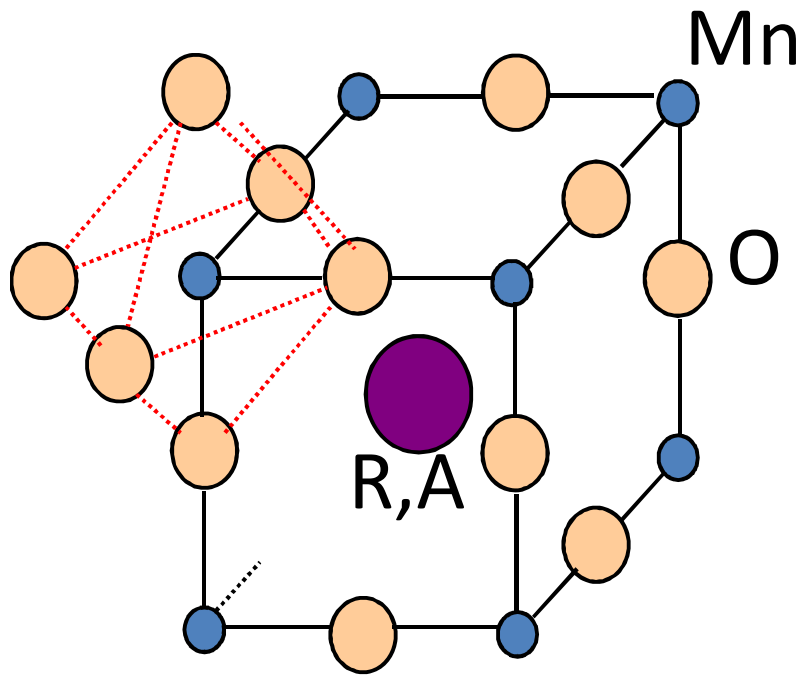
# About Colossal Magnetoresistance (CMR) Manganites



R=La,Nd..

A=Ca,Sr..

Highly explored material in bulk and thin film form in the field of **Spintronics and magnetic sensors**



R=La,Nd..

3+

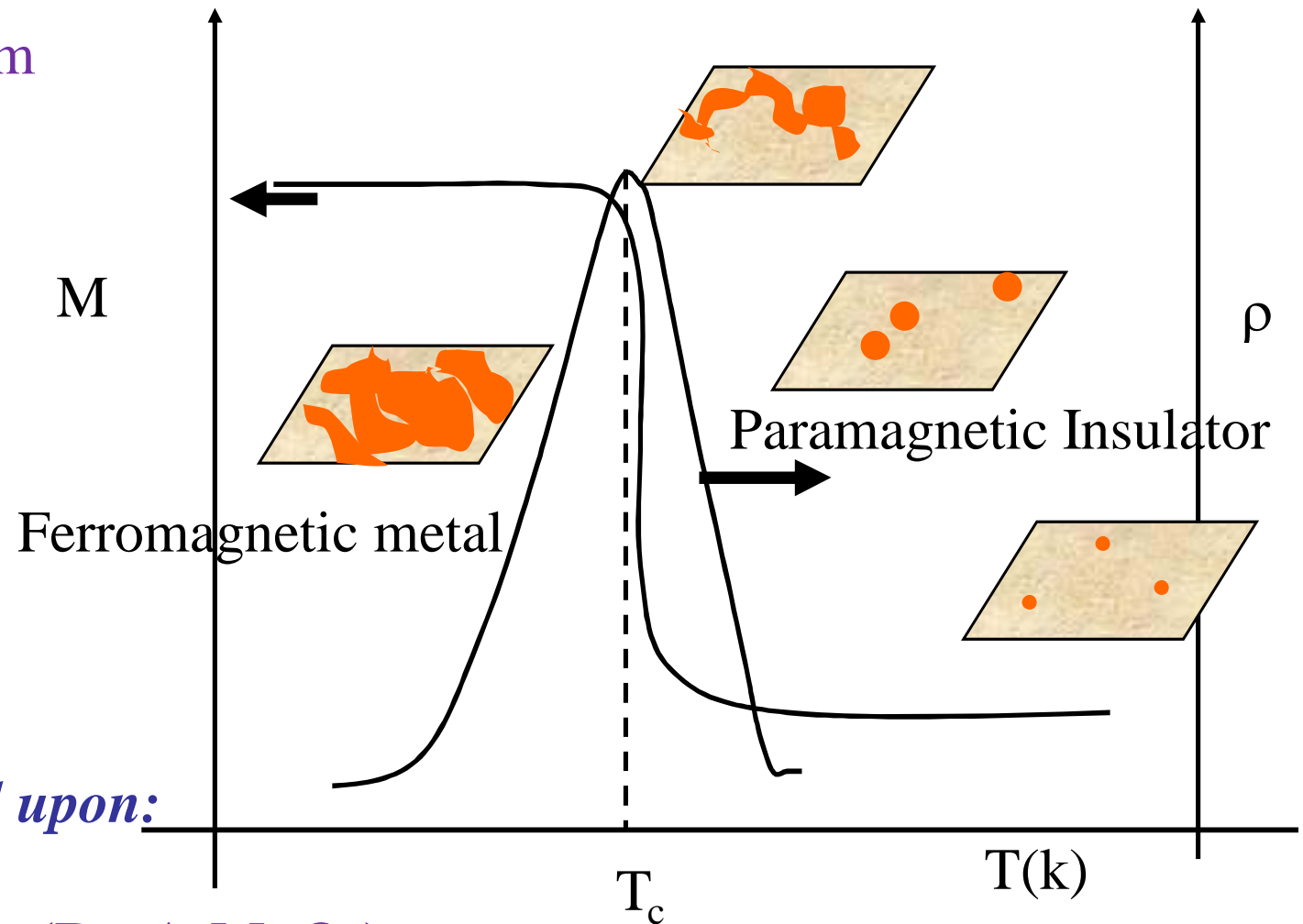


A=Ca,Sr..

2+



## Rich Phase Diagram



### *Properties Depend upon:*

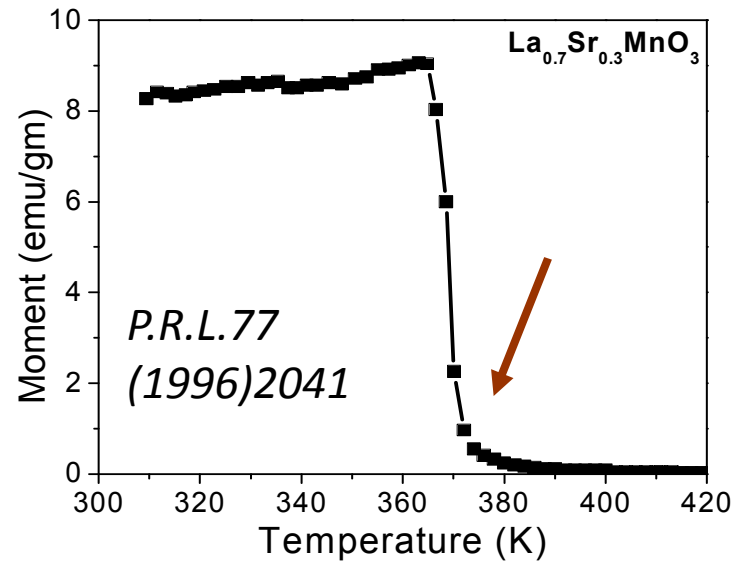
1. Value of x
2. Type of R or A ( $R_{1-x}A_xMnO_3$ )  
R = La, Nd..  
A = Ca, Sr..
3. Tolerance factor
4. Mn Site replacement



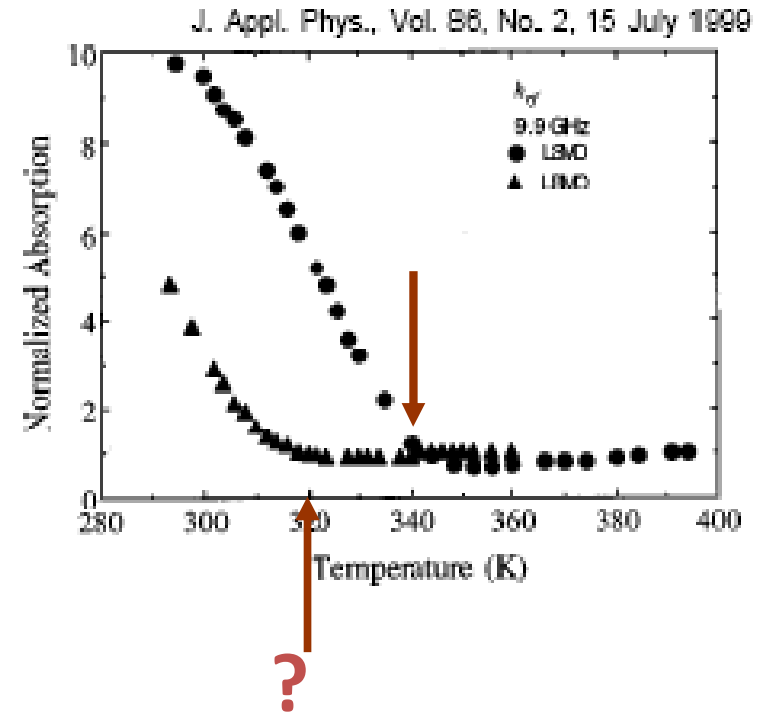
# La<sub>0.7</sub>Sr<sub>0.3</sub>MnO<sub>3</sub>(LSMO) nanoparticles

➔ Curie temperature can be tuned to any desired value depending on the stoichiometric ratio of La:Sr

## Magnetic transition



## Microwave absorption



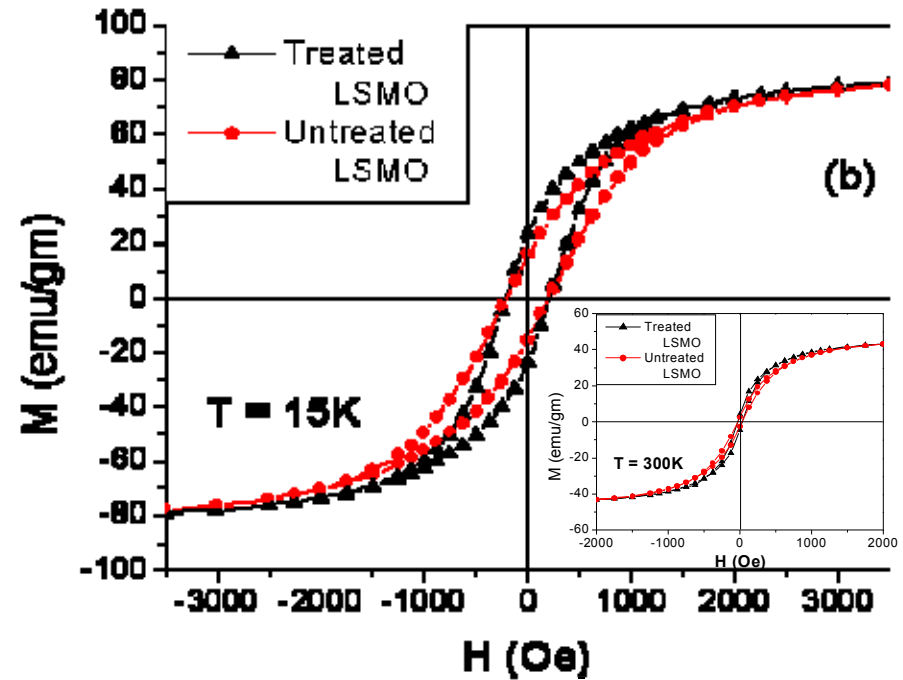
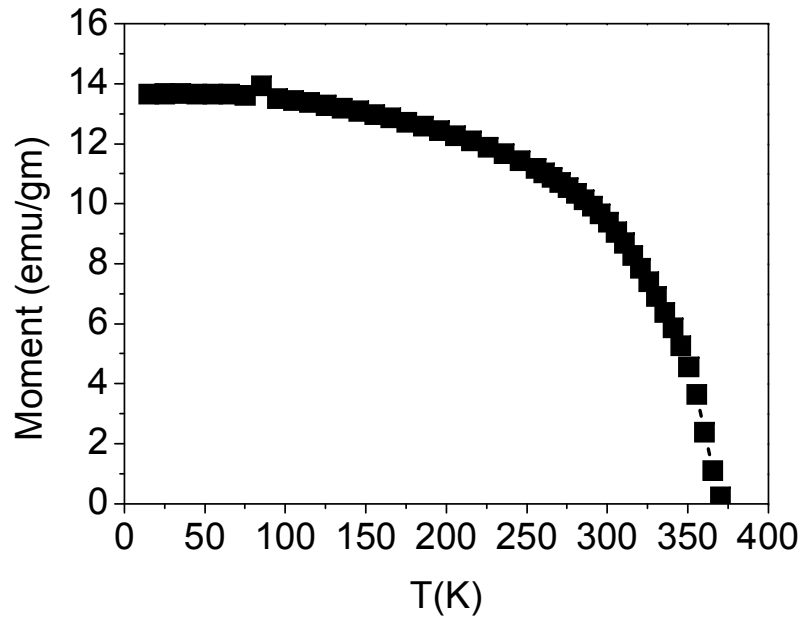


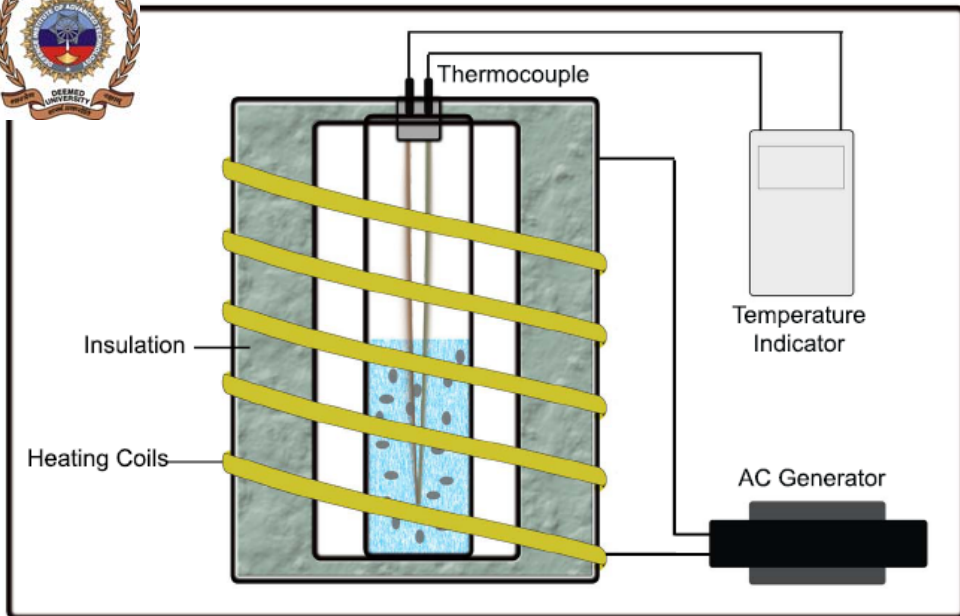


# Characterization results

## Magnetization Data

- ◆  $T_c \sim 360$  K.
- ◆  $M_{sat} \sim 2500$  Oe., Coercivity  $\sim 250$  Oe



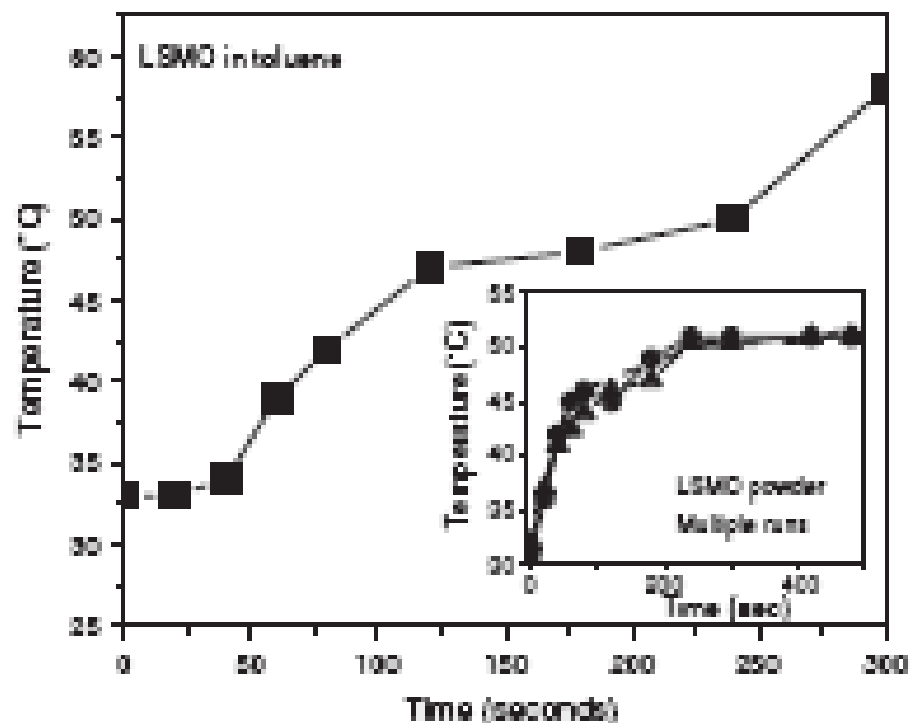


## Microwave (2.45 GHz) absorption result

45°C -120 seconds, 52°C in 200 sec.

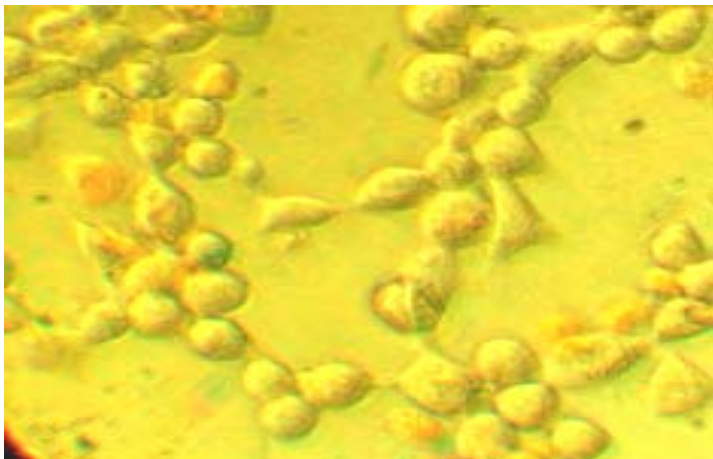
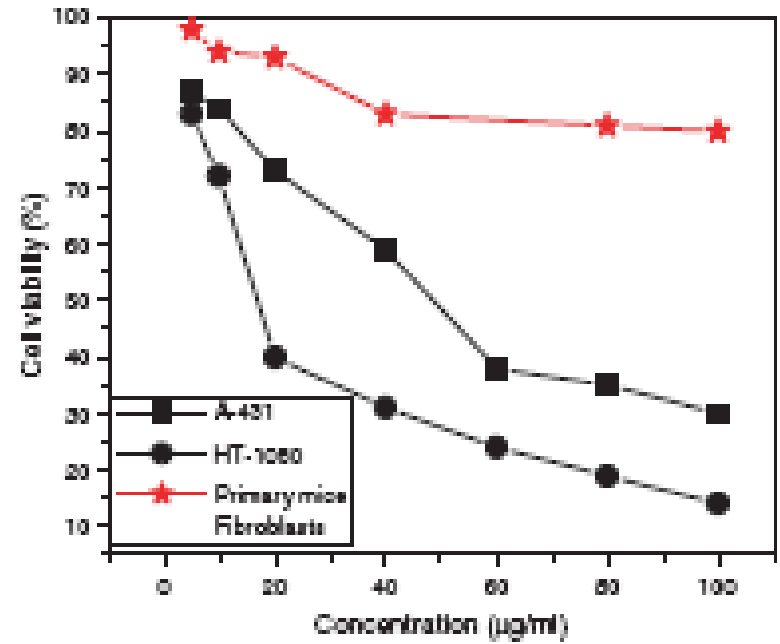


Preliminary setup





# Cytotoxicity





# Conclusions

- LSMO nanoparticles (20-100 nm) evaluated for possible application in hyperthermia.
- Curie temperature  $\sim 360$  K. Exhibit a temperature increase from room temperature to  $45^{\circ}\text{C}$  in 120 s when subjected to microwave exposure of 2.45 GHz.
- Cytotoxicity studies reveal increase in cytotoxicity for larger dosage ( $> 20 \mu\text{g/ml}$ ).



# Controlled approach demanded:

- Narrow Particle size distribution
  - Particles less than 10 nm
  - Particles more than 200 nm

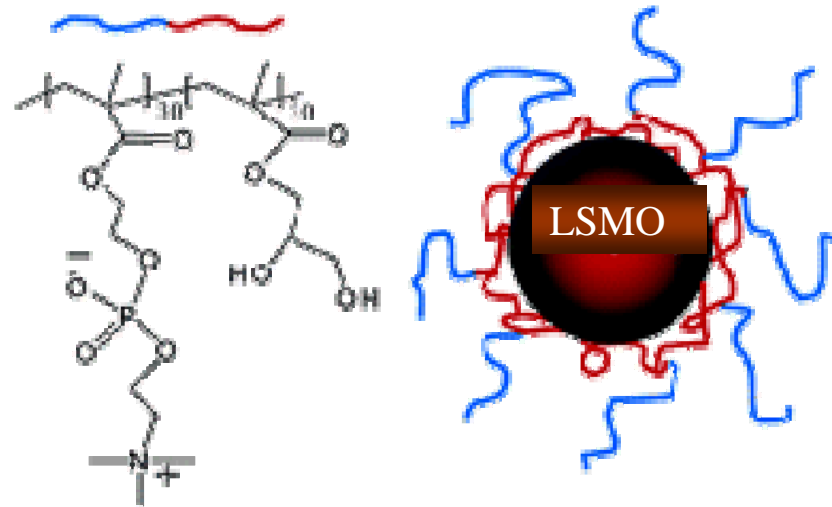
*(J. Magn. Magn. Mater. 2001, 225 17–20,  
Powder Technol. 1996 , 88 267–98)*
- Better cell viability
- Stability during in vivo studies (Leaching studies )
- Agglomeration/clustering
- Work with lower Frequency sources



**Protein and polymer immobilized  
 $\text{La}_{0.7}\text{Sr}_{0.3}\text{MnO}_3$  nanoparticles for  
*hyperthermia* applications**



# Coated Nanoparticles



To get mono-dispersity and non-agglomerated biofriendly nanoparticles:

1. Use of bio-friendly polymer, Dextran
2. Use of protein, Bovine Serum Albumin (BSA) with a linker molecule



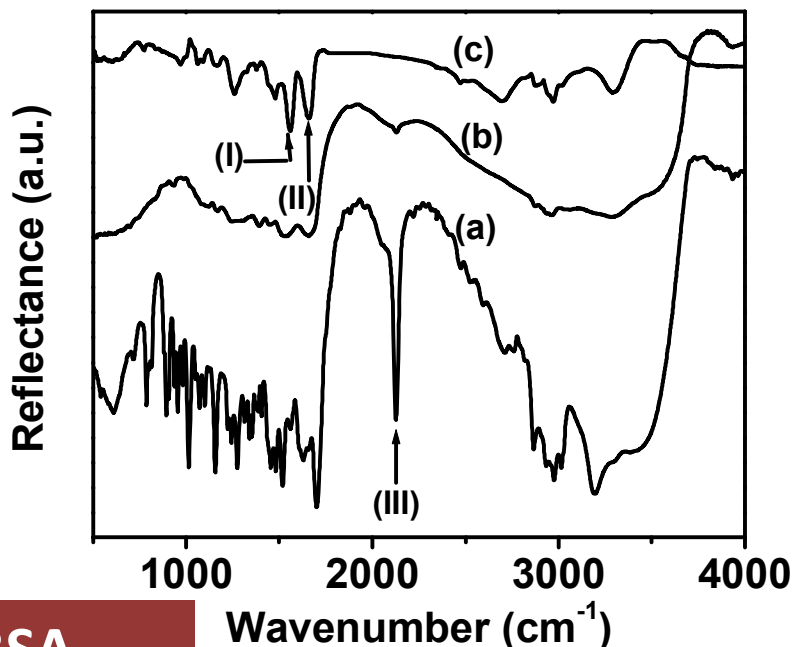
**BSA conjugation:** LSMO NPs were dispersed in 0.005 M phosphate buffer (pH 6.3) and coupling was carried out at an optimized molar ratio of LSMO to CDI

to BSA (2:2:1) with continuous shaking for 24 h. BSA-conjugated manganite NPs were washed by repeated cycles of centrifugation and resuspension in deionized distilled water and finally collected using a magnet and retrieved in dried form by lyophilization. The supernatants were pooled and the total protein concentration was estimated using standard Folin–Lowry method.

**Dextran conjugation:** LSMO NPs (20 mg ml<sup>-1</sup>) were dispersed in 10 ml deionized distilled water and sonicated (400 W, 25 kHz) for 20 min. Dextran was added to this solution in the same concentration (20 mg ml<sup>-1</sup>) followed by sonication for 30 min. The reaction mixture was incubated at room temperature (25 ± 3 °C) for 18 h on a shaker. Similar procedures as described for BSA conjugation were employed for separation and drying of the NPs. Dextran conjugation was confirmed by spectroscopy and magnetization data.

# Biocompatible Conjugation

- (a), CDI,
- (b) BSA
- (c) conjugated



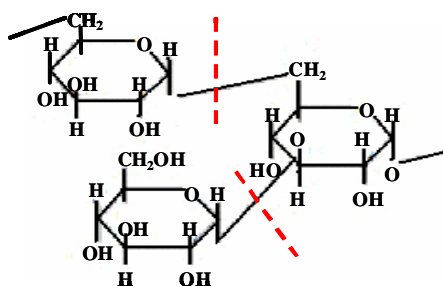
carboxylates -1559  $\text{cm}^{-1}$  peak (feature I) shift to 1661 (II) C=O bond participating in the conjugation.

The 2126  $\text{cm}^{-1}$  (III) in the CDI -(R-N=C) - disappearance in the conjugated system indicates that the  $\text{N}^+$  site serves to provide a crucial link in the manganite-protein conjugation process. LSMO, ( $\text{O}^-$ ) binds electrostatically with the hydrolysed ion at the  $\text{N}^+$  site.

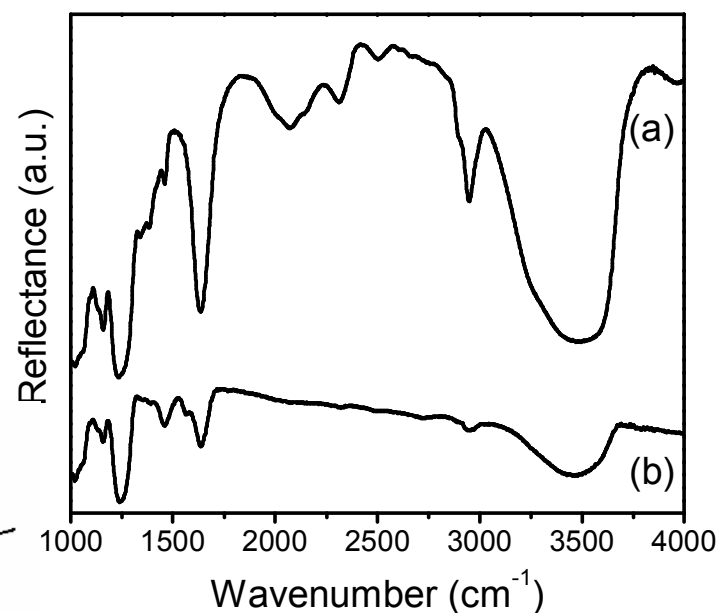
## LSMO:CDI:BSA

1220 (C-O), 1650(C-C), 2500 (O-H), 2950 (C-H) and 3500 (O-H) are also seen in dextran-modified LSMO NPs.

Weakening O-H stretching, we suggest that LSMO binds at this site, either at the 1-6 or 1-3 position of the basic dextran structure.

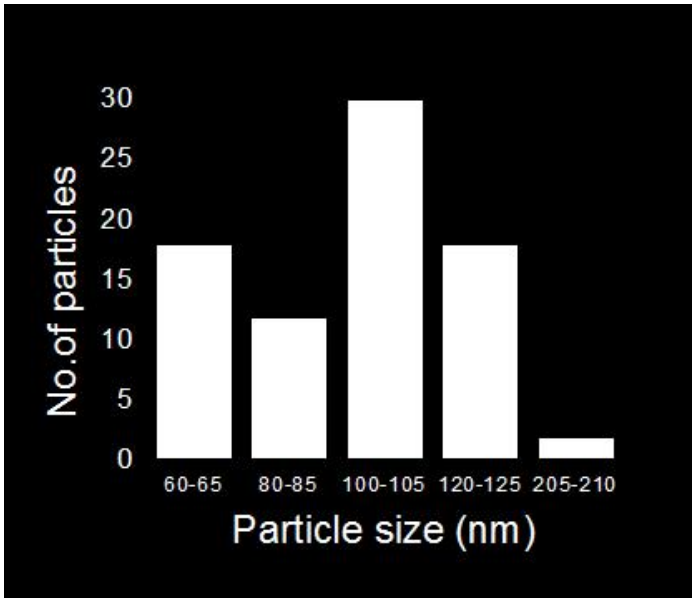
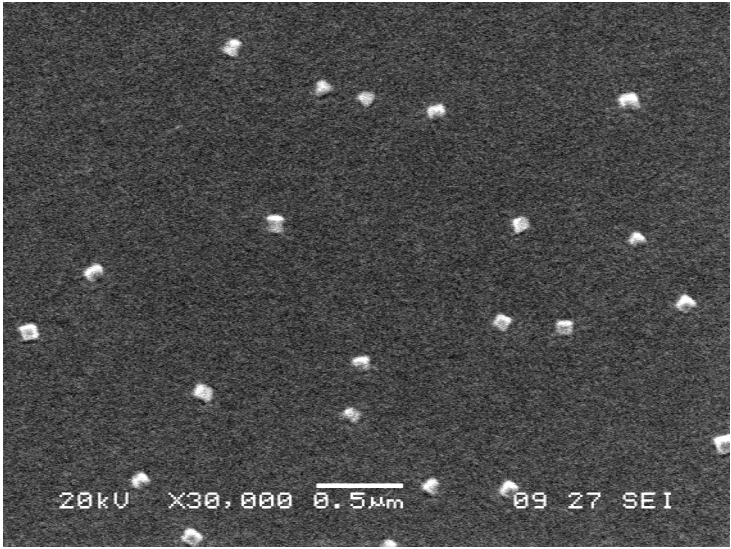


## LSMO:Dextran

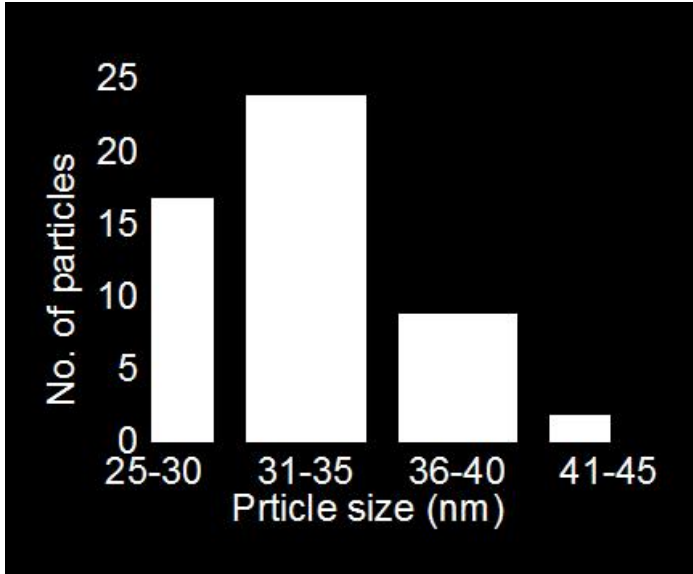
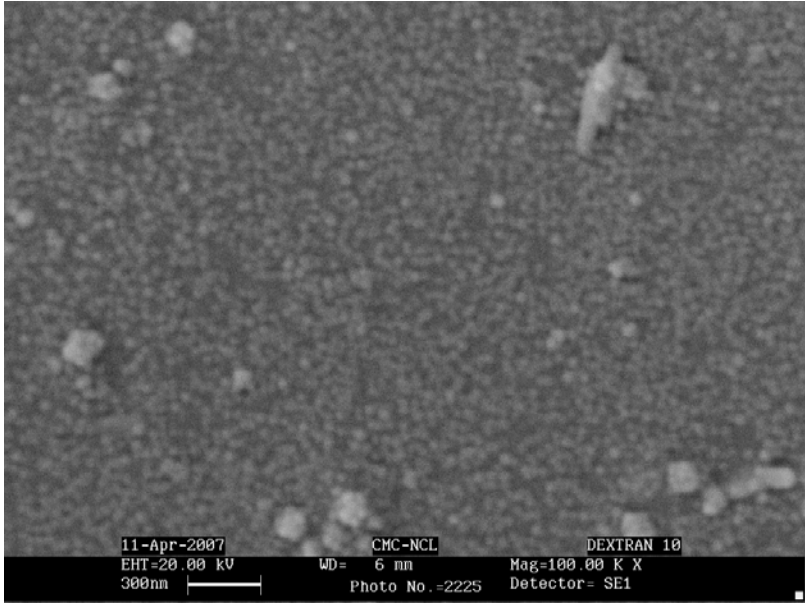




# LSMO:BSA



# LSMO:Dextran



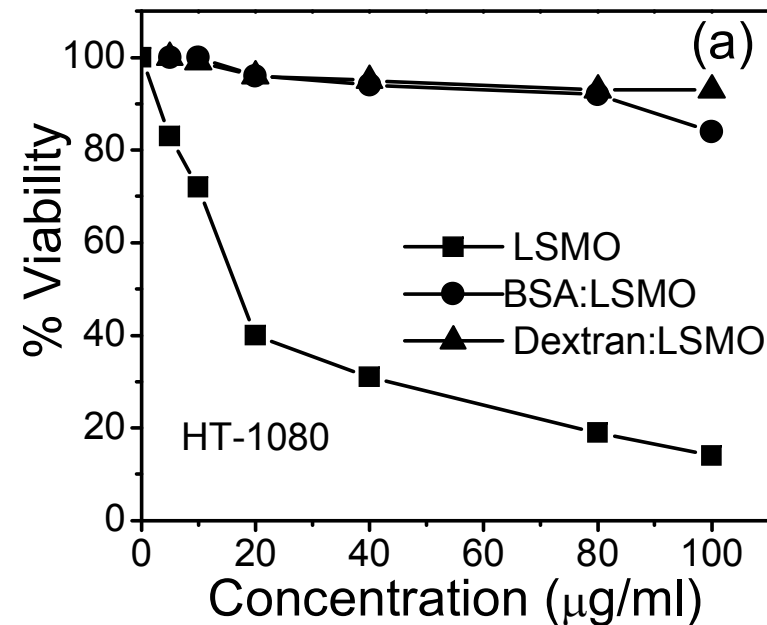
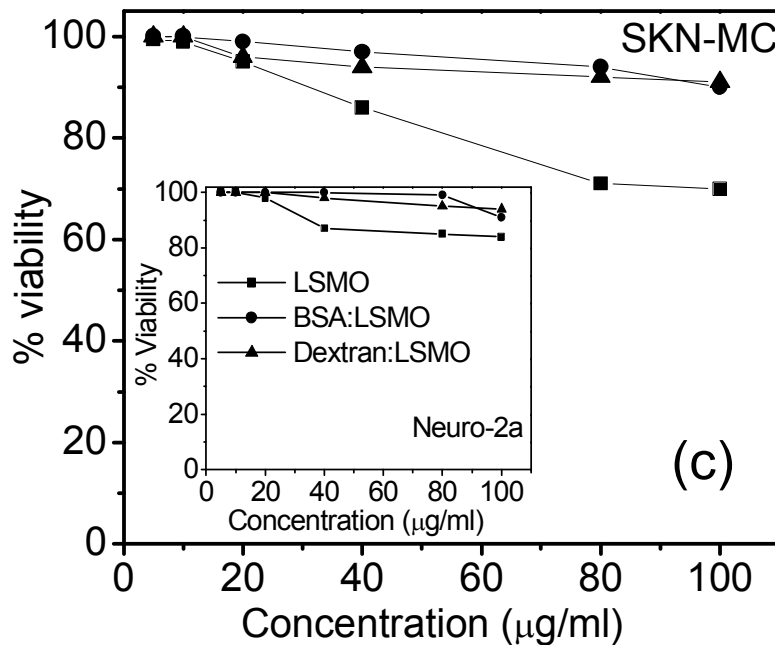
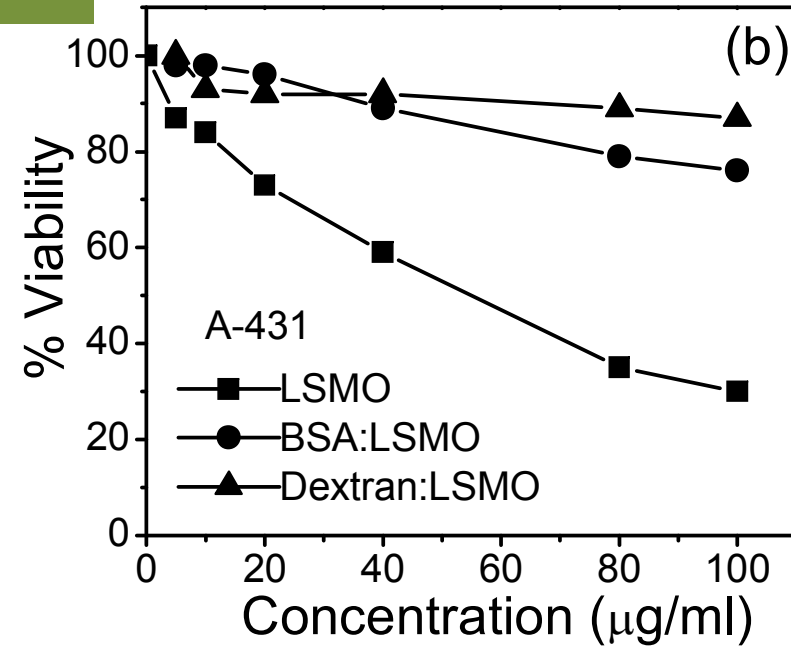


# Cytotoxicity in conjugated systems

Human Fibrosarcoma HT-1080

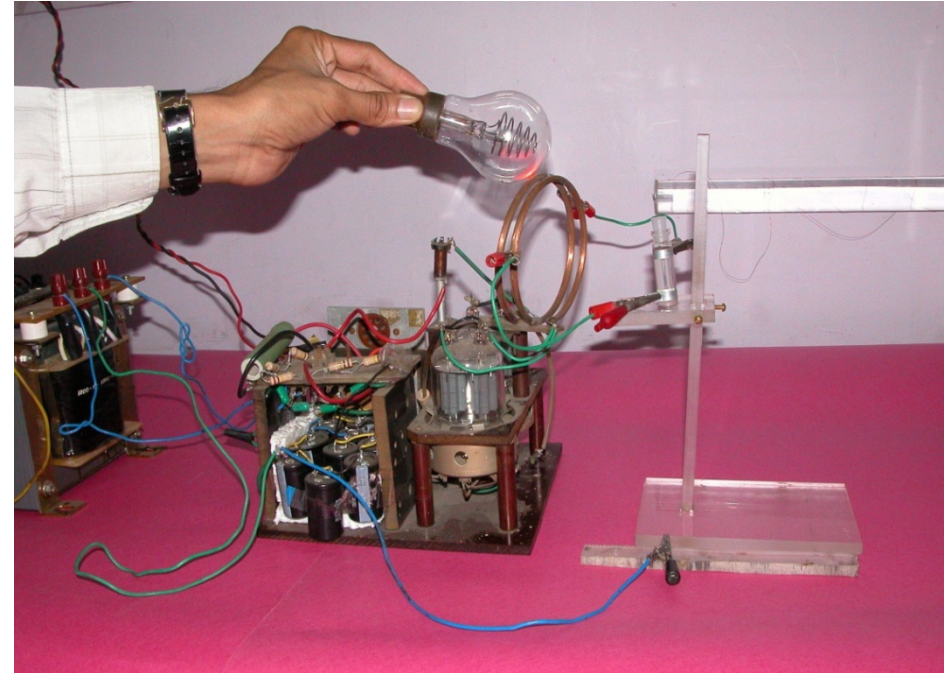
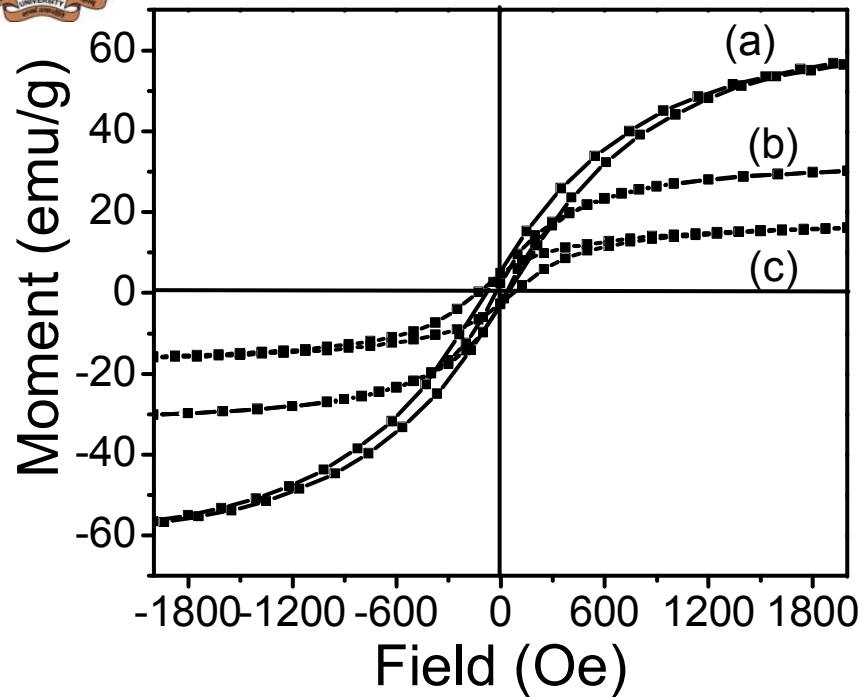
Skin Carcinoma A-431

Human Neuroblastoma SKN-MC



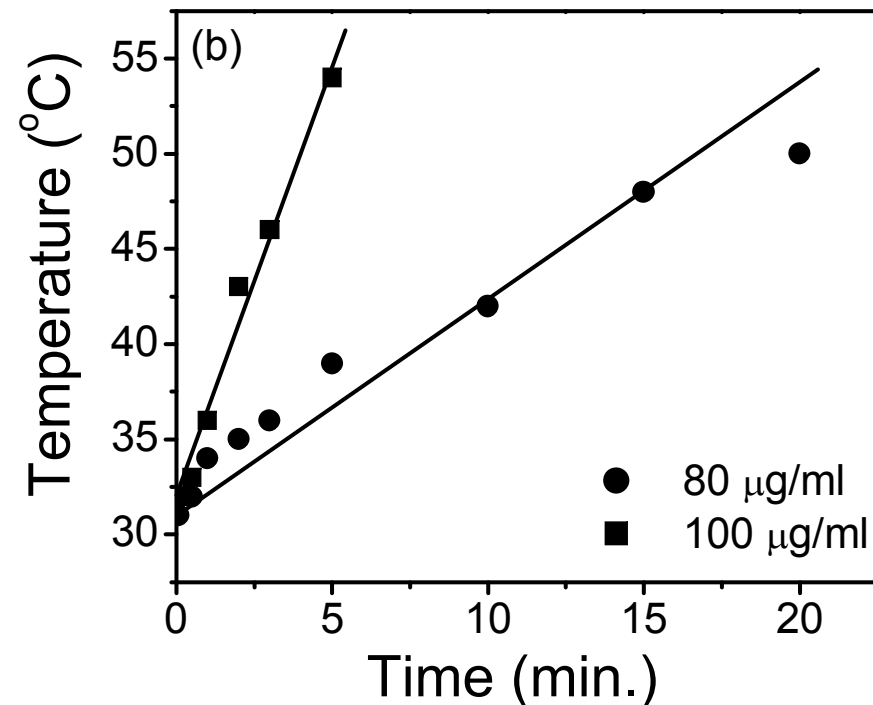
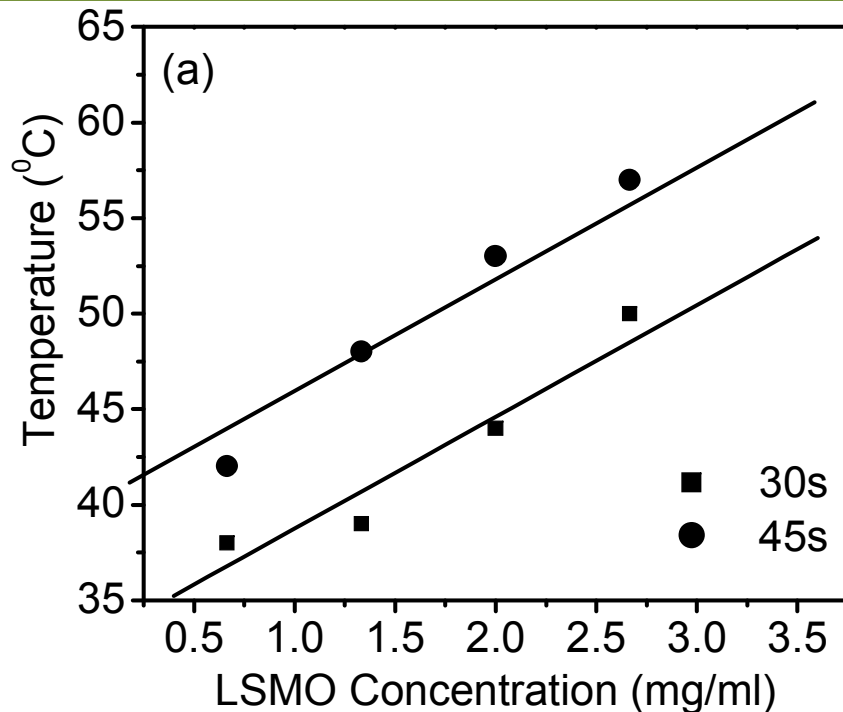


## Setup for RF-heating study



FMR studies have *indicated that maximum energy* will be absorbed by manganite particles at a frequency of a few gigahertz (in-resonance condition). The range of 0.1–20 MHz is thus the off-resonance condition wherein absorption is expected to vary slowly. Thus, although we have performed our experiment at the 20 MHz frequency available to us, we do not expect a significant frequency dependence of the results even if lower frequencies are used

# Radio-Frequency effects in Dextran conjugated systems



Based on our  $\delta T/\delta t$  data, SAR values were found to vary from 0.15 to 16.5  $Wg^{-1}$  depending on the LSMO NPs concentrations in the range of 0.1–12  $mg\ ml^{-1}$  for the applied power of 100 W. A simple calculation shows that an electromagnetic power of 100 W corresponds to a magnetic induction amplitude ( $B_{max}$ ) of  $\sim 8 \times 10^{-4} kA\ m^{-1}$  ( $B_{max} = \text{Sqrt}(2P\mu_0/c)$ , where  $P$  is the power,  $\mu_0$  is the constant of permeability and 'c' is the velocity of light). Gneveckow *et al* have shown that the SAR values increase considerably with increasing magnetic field strength.



## Other concerns

### **Safety of the RF (20 MHz) ... probability that normal tissues may get heated up in this frequency regime?**

~ 5 g quantities of blood and tissue samples - exposed to 20 MHz RF (in the presence and absence of LSMO (5 mg/ml))

Without LSMO increased by only 4°C and with LSMO NPs rose to the level of 48-50°C in 10 min

### **Stability in 'real life' and possible toxicity effects due to leaching of metal ions.**

Mn ions are reported to be neuro-toxic

AAS study showed No leaching of manganese from any of the samples

suggested that LSMO was a highly stable system.



# Conclusions

- Biocompatible molecules such as BSA and Dextran can be effectively immobilized on to LSMO Nanoparticles.
- Dextran conjugated LSMO system shows promising results for hyperthermia applications, as seen from *in-vitro* studies.
- Such bioconjugated Nanoparticles have tremendous application potential, especially in the field of biomedicine.



**Cerium co-doping and stoichiometry  
control for biomedical use of  
 $\text{La}_{0.7}\text{Sr}_{0.3}\text{MnO}_3$  nanoparticles**



## Ce-codoping Effects on Heating Applications

LSMO NPs *doped with cerium* and  $\text{La}_{1-y}\text{Sr}_y\text{MnO}_3$  NPs with *different values of 'y' (La:Sr ratio)* evaluated for toxicity and microwave absorption studies.

### Why Cerium??

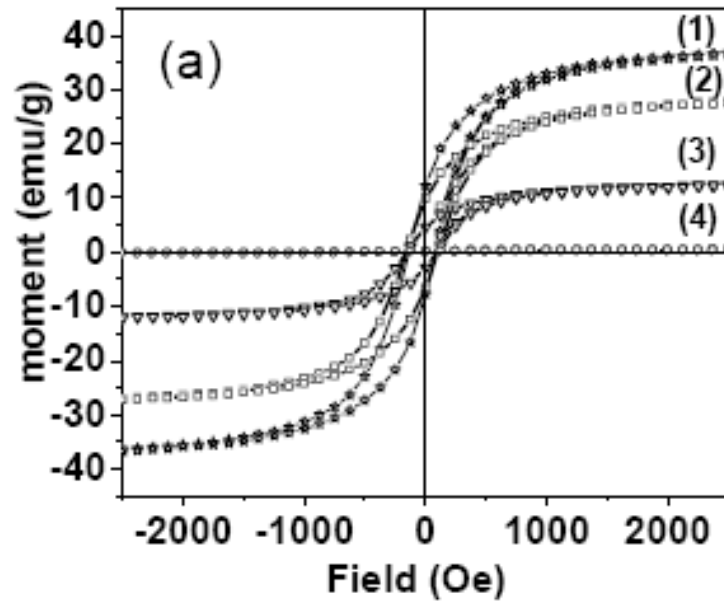
- ⊕ Reported to prevent post-burn sepsis
- ⊕ Provides systematic response by fixing burn toxins and its antiseptic activity

### Why LSMO with La:Sr variation??

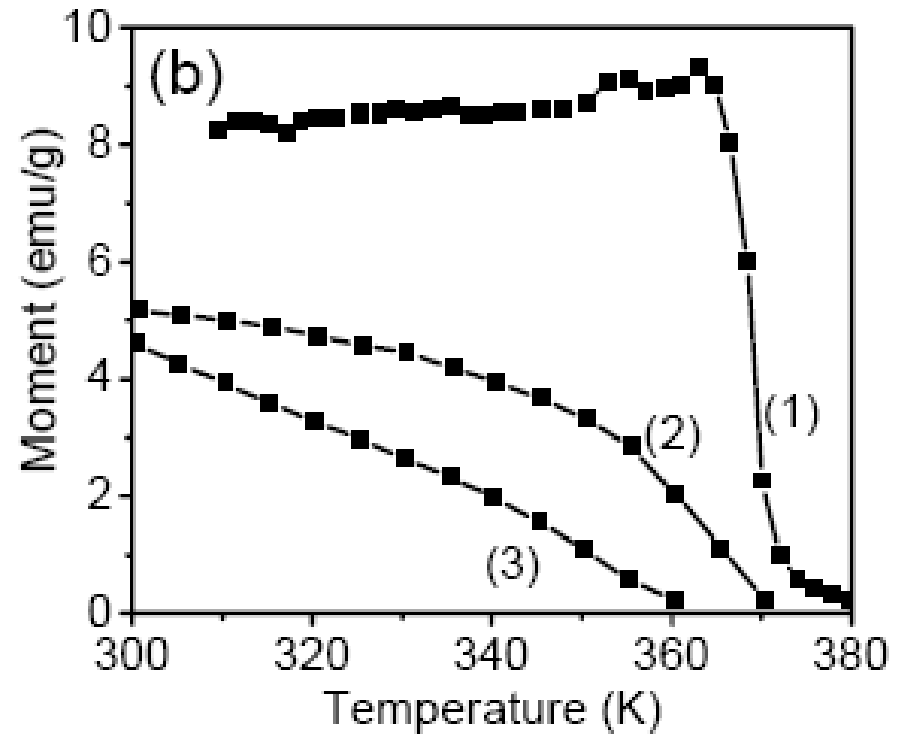
*..... Motivated by some of our observations.....*



# Characterization results



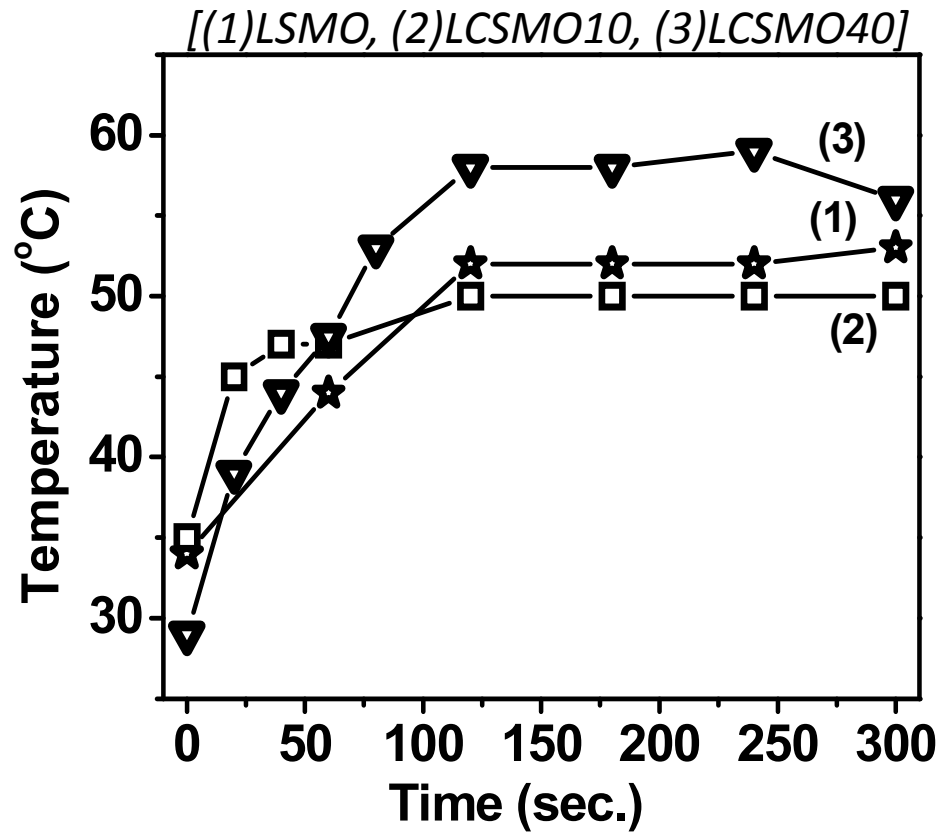
Hysteresis loops for (1) LSMO (2) LCSMO10 (3) LCSMO40 and (4) CSMO samples taken at room temperature.



Dependence of magnetic moment on temperature for (1) LSMO (2) LCSMO10 (3) LCSMO40 samples.



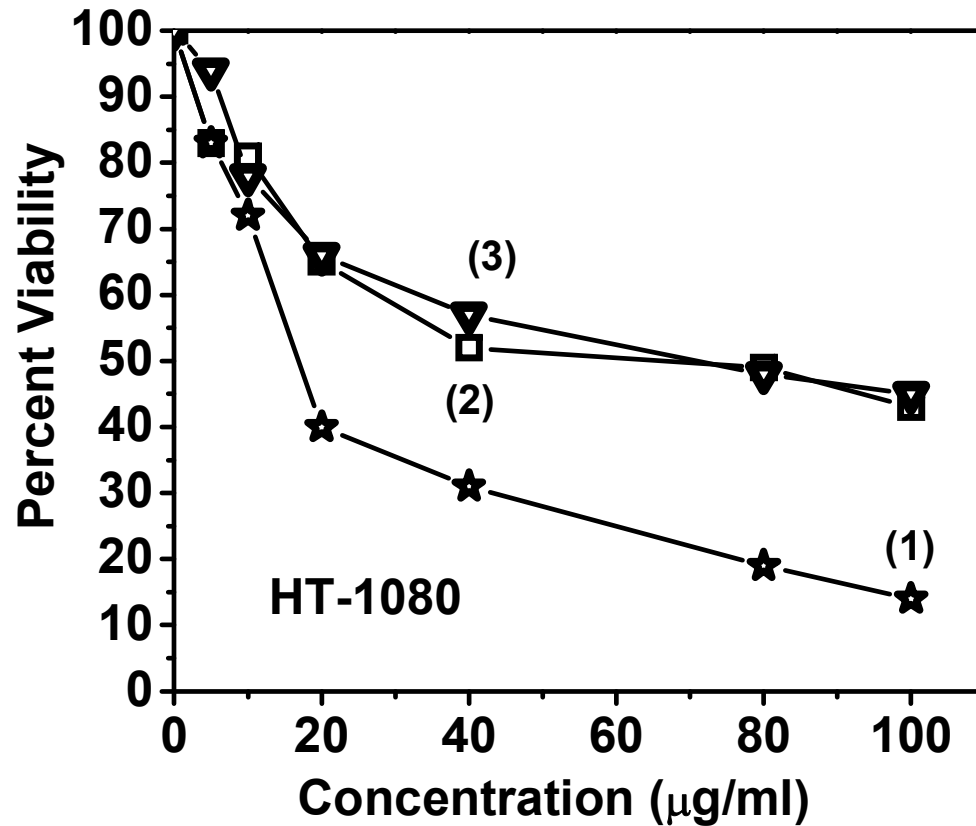
## Microwave absorption (Heating Results)



■ *43-45°C is reached in 60 sec*

■ *52°C in 200 sec.*

## Cytotoxicity studies on human fibrosarcoma (HT-1080) cell lines



■ Cell viability with the dose of 20 µg/ml for

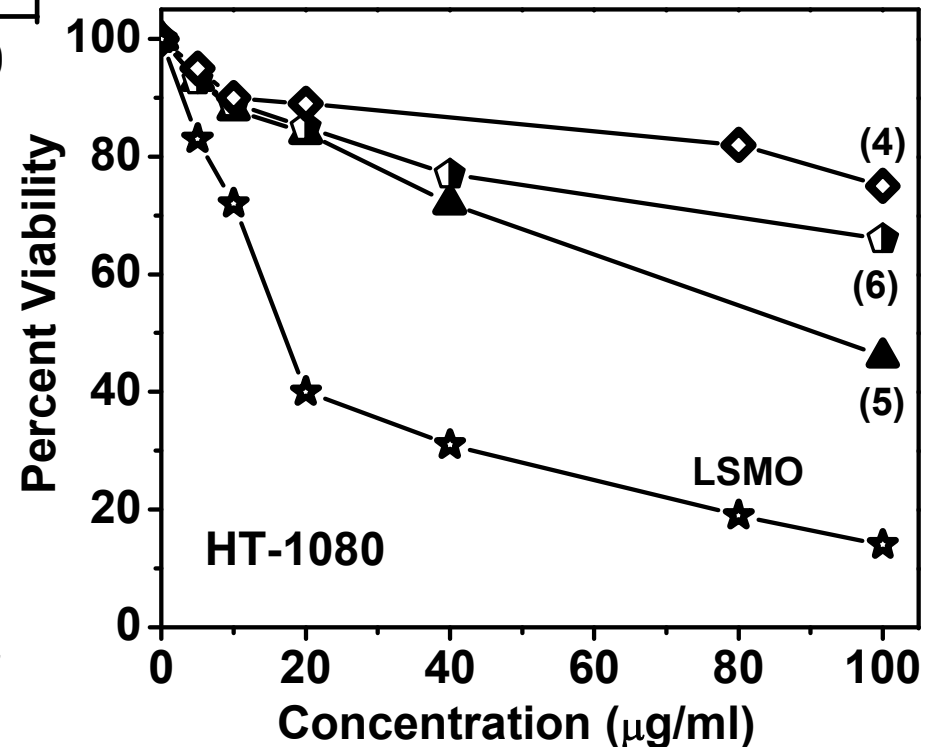
LSMO: 40%

LCSMO10: 68%

LCSMO40: 68%

■ Significant reduction in toxicity due to Cerium incorporation.

[ (4) $La_{0.67}Ce_{0.03}Sr_{0.3}MnO_3$ , (5) $La_{0.5}Sr_{0.5}MnO_3$ , (6) $La_{0.3}Sr_{0.7}MnO_3$  ]



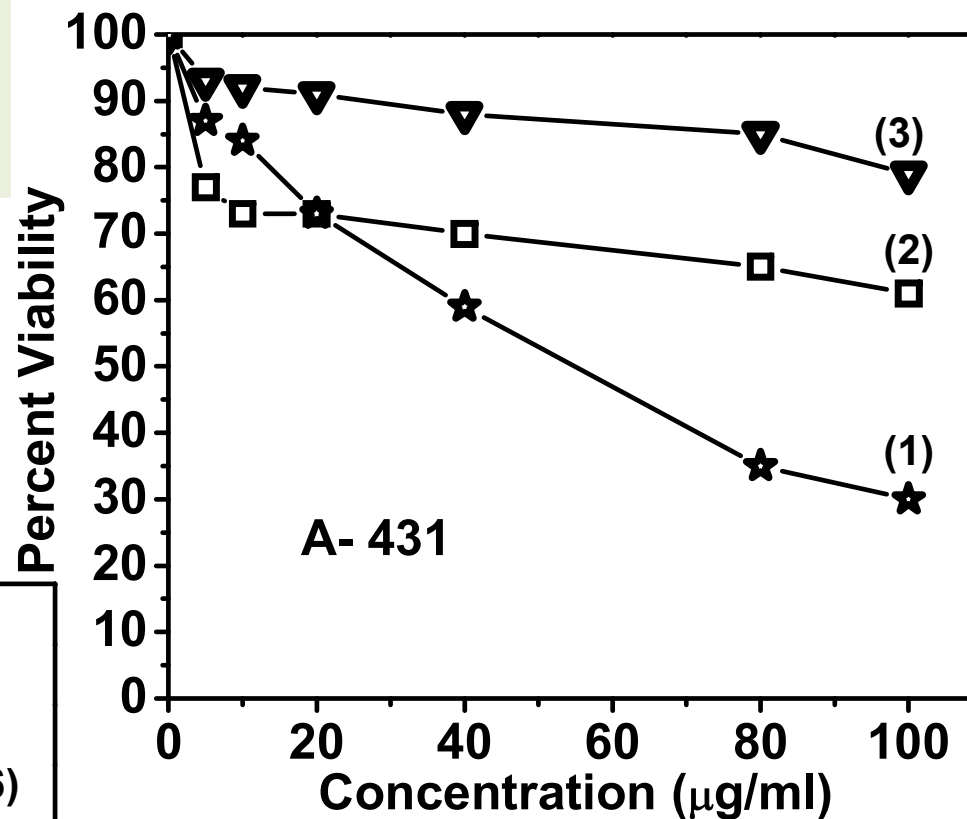
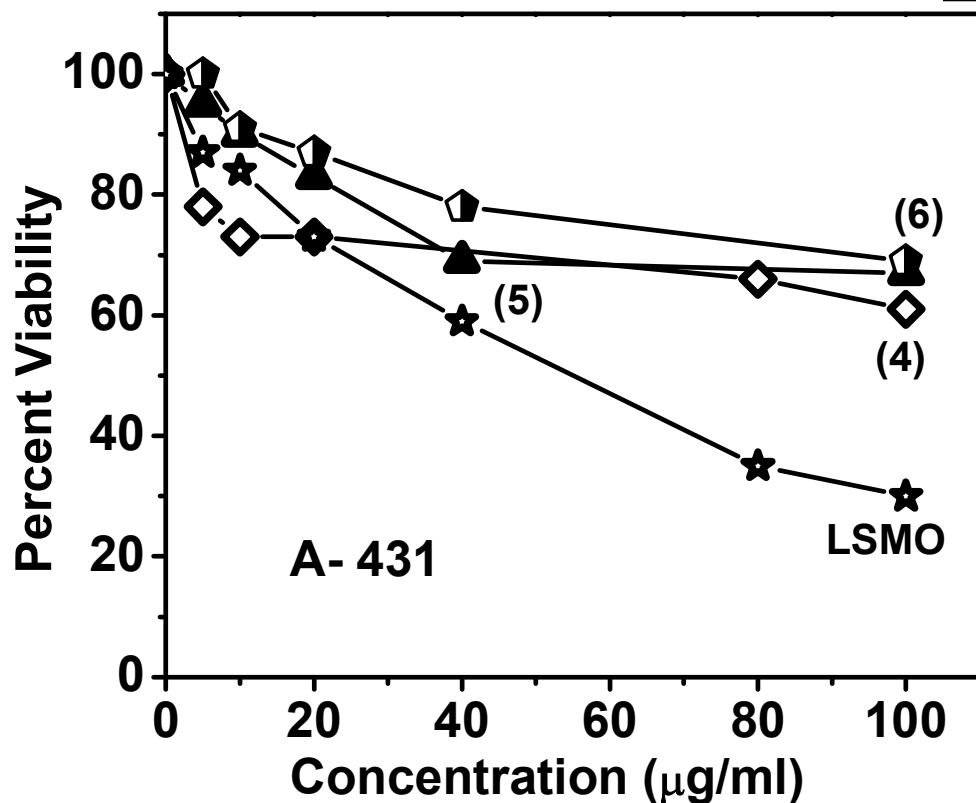
# Cytotoxicity studies on human skin carcinoma (A-431) cell lines

■ Cell viability with the dose of 20 μg/ml for

LSMO: 72%

LCSMO10: 90%

LCSMO40: 90%



■ Significant reduction in toxicity seen due to Ce incorporation.

[ (4)  $La_{0.67}Ce_{0.03}Sr_{0.3}MnO_3$ , (5)  $La_{0.5}Sr_{0.5}MnO_3$ , (6)  $La_{0.3}Sr_{0.7}MnO_3$  ]



# Conclusions

- Cerium co-doping seems to improve the cell viability significantly.
- Stoichiometric control over the La:Sr ratio also exhibits improved cell viability.
- The Ce doping does not alter RF heating results, which are a key to hyperthermia treatments.



# Final Conclusions

**Magnetic nanoparticles are promising candidates for various applications such as :**

Magnetic Hyperthermia

Drug Targeting and Delivery

MRI contrast agents

They can be functionalised with proteins/ amino acids / drugs or site-specific molecules to achieve a particular application regime

**Magnetic nanoparticles made from inorganic materials are by-an-large, non-toxic up-till a particular dosage**

Careful in-vivo studies could demonstrate the actual efficacy of these nanoparticles in actual medicine / therapeutics.



**Thank You...**



## Antioxidants and Cancer

The study of antioxidant use in cancer treatment is a rapidly evolving area. Antioxidants have been extensively studied for their ability to prevent cancer in humans. On use of antioxidants as cancer therapy, number of reports have shown a reduction in adverse effects of chemotherapy when given concurrently with antioxidants.

1. VandeCreek L, Rogers E, Lester J. Use of alternative therapies among breast cancer outpatients compared with the general population. *Altern Ther Health Med* 1999;5:71-76.
2. Singh DK, Lippman SM. Cancer chemoprevention part 1: retinoids and carotenoids and other classic antioxidants. *Oncology* 1998;12:1643-1660.
3. Prasad KN, Kumar A, Kochupillai V, Cole WC. High doses of multiple antioxidant vitamins: essential ingredients in improving the efficacy of standard cancer therapy. *J Am Coll Nutr* 1999;18:13-25.
4. Weijl NI, Cleton FJ, Osanto S. Free radicals and antioxidants in chemotherapy induced toxicity. *Cancer Treat Rev* 1997;23:209-240.

Density functional theory is used to study the antioxidant mechanism of curcumin. Five different mechanisms are considered:

single electron transfer (SET),

radical adduct formation (RAF),

H atom transfer from neutral curcumin (HAT),

H atom transfer from deprotonated curcumin (HAT-D),

and sequential proton loss electron transfer (SPLET).

It is proposed that the curcumin + DPPH reaction actually takes place mainly through the SPLET mechanism, while the reaction with  $\cdot\text{OCH}_3$ , and likely with other alkoxy radicals, is governed by the HAT mechanism.

The calculated overall rate constants for this reaction are  $1.16 \times 10^{10}$  (benzene) and  $5.52 \times 10^9$  (water) -  $\text{L mol}^{-1} \text{s}^{-1}$ ..

Single electron transfer (SET):



Radical adduct formation (RAF):



Hydrogen atom transfer from neutral curcumin (HAT):



Hydrogen atom transfer from deprotonated curcumin (HAT-D)



Sequential proton loss electron transfer (SPLET):

